ORGANIC CHEMISTRY FRONTIERS

REVIEW

View Article Online
View Journal | View Issue

Cite this: *Org. Chem. Front.*, 2024, **11**, 2954

Electrochemical switching in mechanically interlocked molecules (MIMs)

Ayush Bhadani [a,b] and Murugavel Kathiresan *[c]

Mechanically interlocked molecules (MIMs) which include rotaxanes and catenanes are formed by the mechanical linking of two or more components and have significant potential in the construction of molecular machinery owing to their intercomponent dynamics. Synthesis of these mechanically bonded interlocked molecules is delicate due to the inherent entropy constraints required to preorganize structural units for interlocking. However, if accomplished, it offers the advantage of stimuli-responsive behaviour and the control of the rotation/movement of components at the macroscopic level. Currently, synthetic MIMs are transitioning from creating basic architectures to complex architectures with potential functional systems for real-world applications. Switching occurs in different ways in these MIMs, such as chemical (pH, solvent polarity, and guest-induced switching), and electrochemical switching (redox switching). This review looks at some of the most recent studies on electrochemical switching that shows prevalent interest in MIMs among scientists seeking to create functional molecular machines that outperform their natural analogs or possess unique features.

Received 11th January 2024,
Accepted 2nd April 2024

DOI: 10.1039/d4qo00061g

rsc.li/frontiers-organic

Introduction

The term Supramolecular chemistry was initially coined by Nobel laureate Prof. J. M. Lehn in the 1970s, who defined Supramolecular chemistry as "chemistry beyond the molecules".[1] Supramolecular chemistry has become a multi/interdisciplinary field of research with its arms touching the significant branches of science like organic, inorganic, materials, analytical, biological, and environmental chemistry.[2] Its significance can be inferred by the two Nobel prizes given in this subject in 1987 (Donald J. Cram, Jean-Marie Lehn, and Charles J. Pedersen) & 2016 (Jean-Pierre Sauvage, Sir J. Fraser Stoddart, and Bernard L. Feringa) for their works on the advancement of host–guest systems which lead to elementary comprehension of the concepts of intermolecular forces/non-covalent interactions and later for the development of miniaturized nanomachines using the concepts of supramolecular chemistry respectively.[3] These multicomponent structures, which depend on reversible non-covalent interactions for existence, can associate and dissociate in response to external stimuli.[4] Non-covalent interactions comprise electrostatic interactions, pi–pi interactions, hydrogen bonding, metal coordination, charge-transfer complexes, hydrophobic forces, and van der Waals forces (Fig. 1).[5–11] These non-covalent interactions are highly selective with structure specificity.

The concept of intermolecular forces was first put forth by Johannes Diderik van der Waals in 1873. However, it was Hermann Emil Fischer who laid the philosophical groundwork for supramolecular chemistry. Fischer proposed the "lock and key" model of host–guest chemistry and molecular recognition in 1894, which describes the interactions between enzymes and their substrates.[12] Non-covalent bonds were gradually identified in greater detail at the start of the twentieth century after Latimer and Rodebush's description of the hydrogen bond in 1920.[13] These concepts resulted in the understanding of biological processes and protein structure, of which a significant discovery is the double helix structure of DNA, two distinct strands of nucleotides coupled through hydrogen bonds. Based on these understandings, chemists began studying artificial structures based on non-covalent interactions, like micelles and microemulsions in parallel. Further, these concepts were successfully applied to synthetic systems and the advancement came in 1960s with the synthesis of artificial supermolecule, Crown ether that can selectively bind to K^+ ions.[14] Meanwhile, Prof. Cram and Prof. Lehn's group reported the preparation and complexation of spherands and cryptands respectively.[15,16] After these reports, there was a rapid expansion in the field of supramolecular chemistry where new concepts such as interlocked molecules beyond host–guest recognition started to emerge.[17–21]

[a]*School of Chemical Sciences, National Institute of Science Education and Research (NISER), Odisha 752050, India*
[b]*Homi Bhabha National Institute (HBNI), Training School Complex, Anushaktinagar, Mumbai 400094, India*
[c]*Electro Organic & Materials Electrochemistry Division, CSIR – Central Electrochemical Research Institute, Karaikudi – 630003, Tamilnadu, India. E-mail: kathiresan@cecri.res.in*

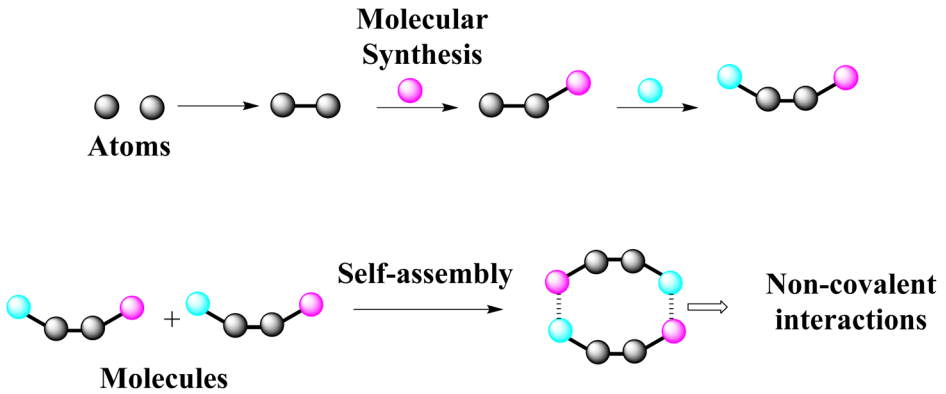

Fig. 1 Cartoon representation of non-covalent interactions.

Recently, the development of new materials and technologies with applications in energy storage,[22,23] catalysis,[24,25] sensing,[26,27] and more has shown a great deal of interest in supramolecular. Recent research has demonstrated that electrochemical formation of supramolecular polymers allows precise control over their structures, properties, and responsiveness to external stimuli.[28–30] Additionally, supramolecular assemblies with electroactive components have drawn lot of attention due to their potential use in energy storage and electronic devices. Researchers have improved charge transport,[31–33] electrochromic behavior,[34–36] and electrocatalytic activity by integrating redox-active molecules or metal complexes into supramolecular structures.[37–40] The creation of next-generation electrical and energy conversion devices is possible with the help of these electroactive supramolecular structures. Advanced electrode materials for energy storage devices like batteries and supercapacitors have been created using supramolecular chemistry to improve the electrode materials' stability and electrochemical performance.[41,42] For instance, ion transport kinetics,[43,44] energy density,[45,46] and cycle life can all be enhanced by functionalizing electrode surfaces with supramolecular host–guest systems.[47]

Overall, integrating supramolecular chemistry with electrochemistry has opened up exciting avenues for designing and

Ayush Bhadani

Ayush Bhadani is presently pursuing his Integrated Master's program in Chemistry at the National Institute of Science Education and Research (NISER) in Bhubaneswar, India. As part of his M.Sc. research, he is concentrating on supramolecular chemistry, specifically in synthesizing water-soluble and light-responsive coordination cages using Pd(II) metal.

Murugavel Kathiresan

Dr Murugavel Kathiresan graduated from the University of Madras with both Bachelor's (2004) as well as Master's degrees (2006), and received his Ph.D. from the University of Osnabrück, Germany, in 2010 under the guidance of Prof. Lorenz Walder. He then moved to the University of Basel, Switzerland, to conduct his post-doctoral research with Prof. Marcel Mayor. He was awarded the DST-INSPIRE Faculty Award in December 2013. From March 2014 to April 2017, he worked as a DST-INSPIRE faculty, since April 2017, he has been working as a Scientist and currently, he is a Senior Scientist at the Electro Organic & Materials Electrochemistry Division, CSIR-Central Electro Chemical Research Institute, Karaikudi, India. His current research interests include viologen-based supramolecular chemistry, along with the investigation of their applications towards photophysical applications, electro-organic synthesis, electrochemical CO_2 reduction and conversion to useful organics, metal–organic frameworks, and porous organic polymers for sensing and energy-related applications.

developing functional materials, devices, and sensing platforms. These advancements hold promise for addressing critical challenges in energy storage, catalysis, sensing, and other fields. They might stimulate the emergence of sustainable and more effective technologies. The focus of this review is to give an overview about electrochemically switchable supramolecular systems. An in-depth discussion on the host–guest interactions in systems such as catenanes, rotaxanes are discussed in detail.

Mechanically interlocked molecules

Mechanically interlocked molecules (MIMs) are molecules that are bound together by mechanical bonds. Rotaxanes, borromean rings, catenanes, and molecular knots are few examples of mechanically interlocked molecular architectures. The synthesis of such intertwined architectures has become more successful with the integration of supramolecular chemistry with conventional covalent synthesis; nonetheless, mechanically interlocked molecular architectures differ from covalently bound molecules and supramolecular assemblies in several aspects. A mechanical bond is the connection that develops between the components of molecules that are mechanically interlocked. Non-covalent interactions are stronger in a mechanically interlocked molecular architecture than they are in a non-mechanically connected one. When exposed to different environmental stimuli such as redox potentials, pH, temperature, solvent nature, *etc.*, MIMs respond, *i.e.*, they move in a variety of ways. Typically, the mechanical motions are driven by reversible non-covalent interactions that are promoted by external stimuli. Recently, MIMs were incorporated into solid-state platforms such as metal organic frameworks and covalent organic frameworks and their applications in optoelectronics, water desalination, and drug delivery were highlighted.[48] Furthermore, Stoddart and co-workers reported the production of poly[*n*]rotaxanes with progressively greater energies by using artificial molecular pumps to provide rings in pairs through cyclical redox-driven processes, all while following the principles of supramolecular chemistry.[49] In a recent review, Stoddart and co-workers has summarized the nature of interactions, synthesis, mechanochemistry and the use of these MIMs in various fields.[50]

Rotaxanes

Rotaxanes are class of mechanically interlocked molecules (MIMs), having unique molecular architecture where macrocycle has been attached onto a linear molecular axle with bulky stoppers at each end. This structure imparts specific properties to rotaxanes, including low bond dissociation energy and susceptibility to external stimuli, like changing pH, vibrations, emitting light energy, removal/addition of electrons, and, *etc.*[51–54] Rotaxanes typically use redox-active groups incorporated into the thread or the macrocycle as the mechanism for electrochemical switching. When an electric potential is applied, these redox-active groups can experience reversible redox reactions that alter their oxidation state and charge. A switchable molecule must exhibit different levels of affinities for a second species in its reduced and oxidized states. As a result, the combination between the receptor and a guest species is thermodynamically stable depending on its oxidation state. In such a system, the differential interaction is often entirely electrostatic. It is necessary for the receptor, the guest, or both to be redox active. A guest or an electrochemically switchable receptor must meet similar conditions. Such a system requires a redox-active component that interacts strongly with the binding element and displays reversible heterogeneous electron transfer kinetics.[55] The rotaxane group must exhibit a redox active group, like ferrocene,[56,57] or viologen units,[58,59] that have different binding stabilities upon electrical stimuli or reduction/oxidized form. These groups can accept/donate electrons providing a redox active system. However, due to attractive interactions or steric effects, the ring often occupies a preferred binding position (station) on the thread without an applied electric potential. The system is stable in this arrangement because the redox-active groups are in a specific oxidation state. The rotaxane system undergoes a redox reaction when an electric potential is applied. By absorbing electrons from an external electrode, the redox-active group, for instance, can be reduced if it is initially oxidized. On the other hand, if the group is initially reduced, it can oxidize by giving electrons to the electrode. The redox reaction changes the redox-active groups' charge distribution and electronic facets. This shift in charge or electrical state might cause the ring and thread's captivating interactions to become weaker or more robust. Consequently, depending upon the oxidation state of the redox-active groups, the ring can be pushed to a different binding site (station) along the thread. The redox-active groups return to their initial oxidation state when the supplied electric potential is removed, stabilizing the ring's new position on the thread. Until applying a different electric potential, this new condition is stable.

Electrochemical switching of MIMs

Rotaxanes and catenanes are types of mechanically interlocked molecular architectures (Fig. 2). In case of rotaxane and catenane they thread one molecular component through another, resulting in unique properties and functionalities. Rotaxanes consist of a linear molecular component called an "axle" or "thread" threaded through a macrocyclic element referred to as a "ring" or "wheel".

The axle and ring are held together by noncovalent interactions including hydrogen bonding and coordination interactions. Crucially, the large stoppers or groups at the edges of the axle on rotaxanes which prevents the ring from dissociating. The threaded ring can move along the axle but cannot be completely detached.[60,61] While, catenanes comprise two or more interlocked macrocycles, called rings or cycles, akin to

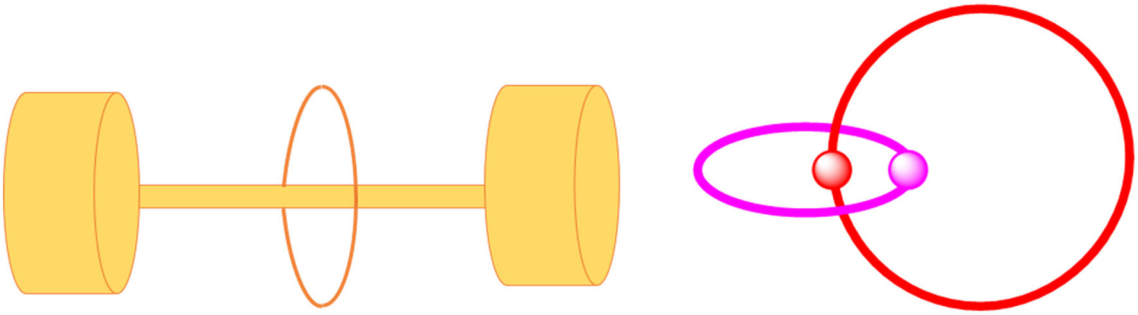

Fig. 2 Cartoon depicting rotaxanes (left), catenanes (right).

the methodology employed in crafting other mechanically connected molecular structures like interlocked rings (catenanes) and rings threaded onto molecular axles (rotaxanes)[62,63] Unlike rotaxanes, catenanes do not have a linear component threaded through a macrocycle; instead, they consist of two or more rings linked together topologically (Fig. 2). The interlocking can occur in various ways, such as a simple ring threading through another or two rings intertwining. Catenanes typically do not have stoppers or groups to prevent dissociation between the rings.[64,65]

Mechanism for electrochemical switching in rotaxanes

The driving force for the electrochemical switching in rotaxanes is the change in Gibbs free energy (ΔG) associated with the redox reactions of the electroactive groups. The Gibbs free energy change can be related to the potential difference (ΔV) applied across the system using the equation:

$$\Delta G = -nF\Delta V$$

where n is the number of electrons transferred in the redox reaction, and F is the Faraday constant.

The position of the ring on the thread is determined by the binding energies between the ring and different binding sites (stations) along the thread. Denoting the binding energy at a particular station as E_i, where i represents the station index. The probability of finding the ring at a specific station depends on the relative binding energies. According to the Boltzmann distribution, the probability (P_i) of the ring being at station i is given by:

$$P_i \propto e^{\left(-\frac{E_i}{kT}\right)}$$

where k is the Boltzmann constant, and T is the temperature.

The redox-active groups in the rotaxane undergo reversible redox reactions, changing their oxidation state and charge. The redox reactions are driven by the applied potential difference (ΔV) and are described by the Nernst equation:

$$E_i = E_i^o + \left(\frac{RT}{nF}\right)\ln\left(\frac{[Ox]}{[Rd]}\right)$$

where E_i is the potential at station i, E_i^o is the standard potential at that station, [Ox] and [Rd] are the concentrations of the oxidized and reduced forms of the redox-active group, R is the gas constant, and [Ox]/[Rd] represents the ratio of the oxidized and reduced species concentrations.

The minimum free energy state determines the equilibrium position of the ring on the thread. At equilibrium, the sum of the free energy contributions from the binding energies (E_i) and the redox reactions (ΔG) is minimized.

$$\sum [P_i \times (E_i + \Delta G)] = \min$$

here, the probability-weighted sum of the binding energies and the free energy change associated with the redox reaction is minimized.

The equilibrium position of the ring can be calculated by numerically solving the optimization problem. This involves iterating through different potential values (ΔV) and calculating the probabilities (P_i) and the corresponding free energy contributions. The potential that minimizes the free energy is the equilibrium potential, and the corresponding probabilities give the equilibrium distribution of the ring along the thread.

By manipulating the potential difference applied across the rotaxane system, one can control the redox reactions, which affect the binding energies and the equilibrium distribution of the ring. This enables the electrochemical switching of the ring's position in the rotaxane. The mathematical model described here provides a simplified framework for understanding the principals involved in the electrochemical switching mechanism. Still, existing systems can involve additional factors, such as solvent effects and non-ideal behaviour, which may require more rigours mathematical descriptions.

Recently, extensive work has been done on interlocked molecules under the umbrella of the Ratchet mechanism, especially by Leigh,[66,67] and Stoddart,[68–70] Credi,[71–73] and others.[74–77] For example, in two independent studies Stoddart and coworkers, show electrochemical switching through ratchet mechanism.[78,79] Herein, they showed the synthesis (Fig. 3a), and functioning of a linear molecular pump, crafted as an intermediate [2]rotaxane. It is formed through the controlled threading (under redox/thermal influence) and unthreading (also under redox/thermal control) of a $CBPQT^{4+}$ ring along a molecular dual pump (MDP^{6+}) dumbbell. The

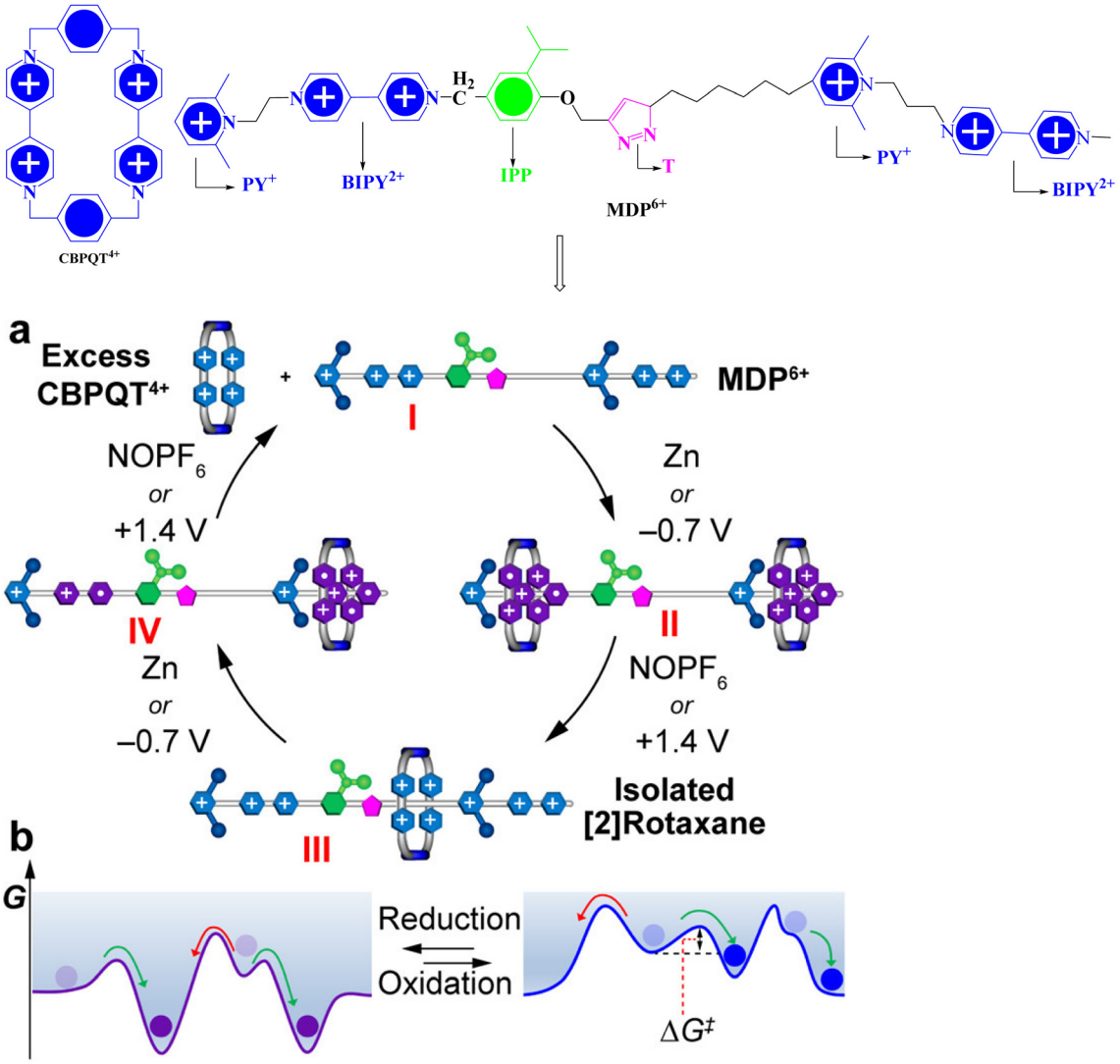

Fig. 3 Stoddart's artificial molecular dual pump. Reproduced with permission from ref. 79, Copyright 2019, American Chemical Society.

action of this dual pump uses an energy ratchet mechanism, achieved by adjusting noncovalent interactions and leveraging redox switching properties in both components. Initially, $CBPQT^{4+}$ and MDP^{6+} exhibit strong repulsion, which is transformed into strong attraction upon reduction of $BIPY^{2+}$ units to $BIPY^{+\bullet}$ units, facilitating the development of stable trisradical tricationic complexes (stage II, Fig. 3b). Subsequent oxidation separates these complexes due to coulombic repulsion. One $CBPQT^{4+}$ ring undergoes rearrangement to form a stable [2]rotaxane, while the second simply unthreads (Stage – III, Fig. 3b). A second reduction prompts the remaining [2]rotaxane to form a complex with the terminal $BIPY^{+\bullet}$ unit. (Stage – IV, Fig. 3b) Upon oxidation, the $CBPQT^{4+}$ ring is expelled in the same direction it entered, resetting the energy ratchet. Redox chemistry regulates this, causing the potential energy wells and coulombic barriers to vary. This process facilitates the gradual, unidirectional capture and release of a ring by coordinating two redox cycles and one rearrangement.

In further study, they synthesized [2]rotaxanes using they synthesised the similar ring (Fig. 4a). They demonstrated the corresponding energy profiles as well as the unidirectional transit of a ring onto, along, and finally off the dumbbell (Fig. 4b). Initially, in Stage I, steric interactions with the PcS and strong coulombic repulsions with PY^{+} cause difficulties for the positively charged ring when it tries to thread onto the dumbbell. Subsequently, in Stage II, the coulombic barrier is lowered by a negative potential reduction of −700 mV, which makes it easier for a stable triradical tricationic complex to form. In Stage III, the ring's escape into the bulk solution is impeded by oxidation by a positive potential of +700 mV, which also decreases the ring's contact with the recognition site and reinstates the coulombic barrier from PY^{+}. As a result, the ring must traverse over the IPP steric barrier in order to join the collecting chain. Ultimately, photocleavage of the stopper PcS is caused by UV irradiation in Stage IV, allowing the ring to reenter the bulk solution.

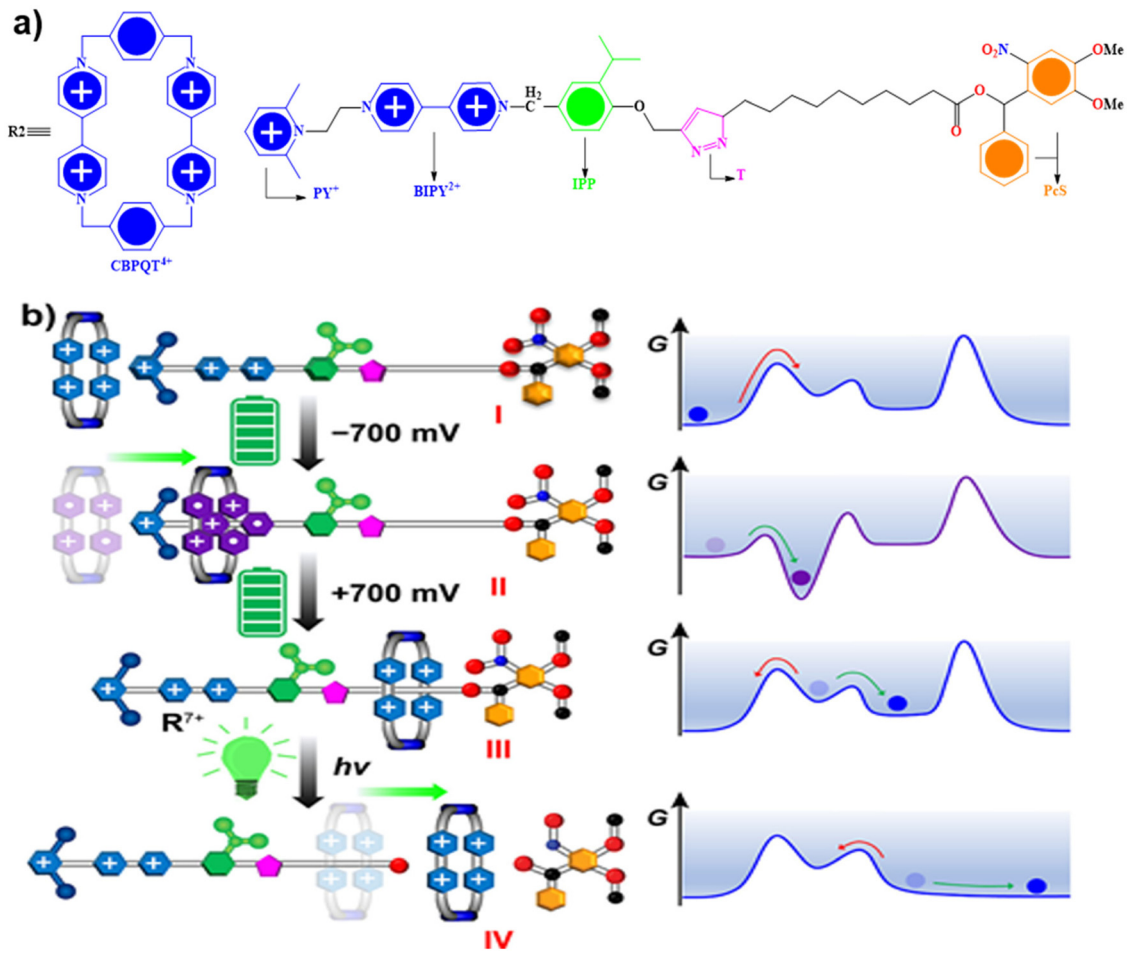

Fig. 4 Stoddart's artificial molecular pump. (a) [2]rotaxane and interlocked ring $CBPQT^{4+}$, (b) ratchet mechanism for shuttling of AMPs (the green and red curved arrows in energy profile diagram represent kinetically favoured and disfavoured transitions, respectively). Reproduced with permission from ref. 78, Copyright 2020, American Chemical Society.

Redox-switching in rotaxanes

The electrochemical switching of rotaxanes changes oxidation states of the molecules due to reversible redox reactions.[80,81] In the presence of electrochemical stimuli, these macrocycles bear large conformational changes and result in a substantial difference in the amplitude of molecular motion (Fig. 5).[82] Moreover, electrochemical changes offer an excellent description of the oxidation state of the central metal atoms,[83] diffusion constants,[84] orbital energies,[85] and electrochemical mechanisms.[86] The electrochemical switching in rotaxanes relies on incorporating redox-active components into the structure. Typically, one or both components—the axle or the ring—contain redox-active units, such as metal centers or organic

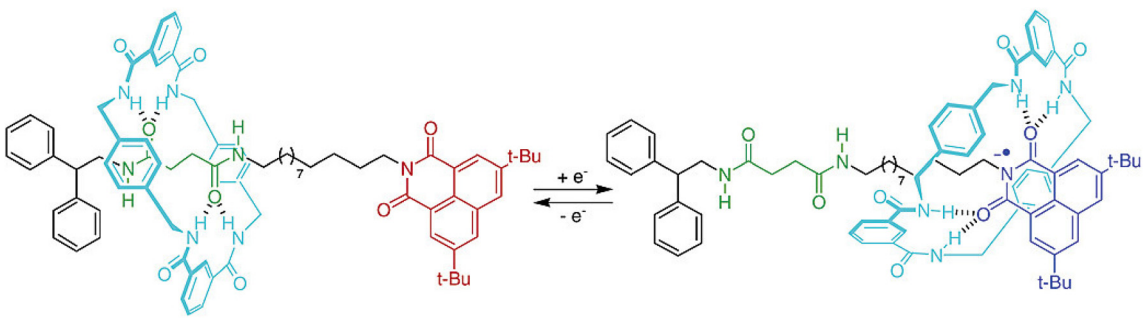

Fig. 5 Electrochemical switching of rotaxane. Reproduced with permission from ref. 91, Copyright 2003, American Chemical Society.

moieties that are capable of undergoing redox reactions.[87] These redox-active units can exist in different oxidation states, which enables the control of the rotaxane's overall electronic condition.[88] Electroanalytical techniques, such as widely used cyclic voltammetry (CV), can measure the variation in the number of isomers in various redox states and convey qualitative evidence for co-conformational alterations *via* altered half-wave ($E_{1/2}$) or peak (E_p) potentials.[89,90] Further information such as shift in peak potentials, reversibility of the system, diffusion coefficients of the complex, association constants, *etc.* can also be determined.

Pioneering work led by Stoddart,[92,93] Sauvage,[94] and Leigh,[95,96] established the effectiveness of electrochemical switching in rotaxanes. For instance, Stoddart and Wasielewski reported the electroswitching of bistable[2]rotaxane in the ground and excited state electronic configuration of BODIPY[53] (Fig. 6).

In this report, they showed that the oxidation of tetrathiafulvalene (TTF) (neutral molecule) to its dicationic state TTF^{2+}, which drives the cyclobis(paraquat-*p*-phenylene) ($CBPQT^{4+}$) towards the BODIPY rotor that substantially increases the quantum yield of BODIPY. Fluorescence becomes more intense due to its high nonradiative rate constant and larger energy barrier caused by its excited-state rotation. After introducing the oxidizing agent $Fe(ClO_4)_3$ (6.25 M), the inherent charge-transfer peak for the TTF unit in the $CBPQT^{4+}$ at 843 nm vanished (Fig. 7a). In contrast, two new absorption bands indicative of the mono-oxidized form of TTF emerged at 450 and 600 nm (Fig. 7b). Additional oxidant addition (up to 2 mol equiv.) caused the mono-oxidized TTF absorbance to vanish and was replaced by an absorption band at 375 nm that indicated the presence of TTF^{2+} dication (Fig. 7c). Later on, the addition of Zn powder (reducing agent) restores all initial absorption bands (Fig. 7d). This restoring of absorption of bands after reduction confirms redox switching where the control unit was $CBPQT^{4+}$ and BODIPY act as the functional unit.

A dumbbell-shaped guest system and rotaxane based macrocyclic host were developed to provide a straightforward and adaptable method for expanding electron catalysis to aid in molecular recognition.[97] The guest $\mathbf{D}^{+(\bullet+)}$ has three components, a 2,6-diisopropylphenyl group on one side of the dumbbell that imparts steric hindrance and prevents the ring from threading, a 2,6-dimethylpyridinium (PY^+) cation on the other side, that functions as a switchable energy barrier in conjunction with a positively charged $BIPY^{\bullet+}$ unit and a $BIPY^{\bullet+}$ unit in the middle of the dumbbell that binds $\mathbf{R}^{2(\bullet+)}$ to form a trisradical complex *via* radical–radical interactions. Initial studies indicate that significant coulombic repulsion causes $\mathbf{R}^{2(\bullet+)}$ to cross over the PY^+ terminal of $\mathbf{D}^{+(\bullet+)}$ very slowly. The energy barrier arising from this repulsive interaction can be modified (Fig. 8a), depending on the charges on the host and guest, by modifying the redox states of the bipyridinium units.

In 2023, Gu *et al.* reported on a tristable [3]rotaxane with redox and photo switchable properties. It was composed of two $CBPQT^{4+}$ macrocycles arranged in a dumbbell shape, with a dioxynaphthalene (DNP) unit between the redox-active tetrathiofulvalene (TTF) and photoactive azobenzene (AB) units.[98] The movement of the $CBPQT^{4+}$ wheels within the [3]rotaxane, labelled as R1, could be initiated by both UV/Vis light exposure and manipulation of the redox states of the TTF unit (Fig. 9).

The two $CBPQT^{4+}$ wheels in R1 predominantly occupied positions adjacent to the TTF and terminal E-AB units, respectively, before they were exposed to light. When exposed to UV (365 nm)/Vis (525 nm) light, the *Z*/*E* photoisomerization of the AB unit-initiated movement, prompting one $CBPQT^{4+}$ wheel

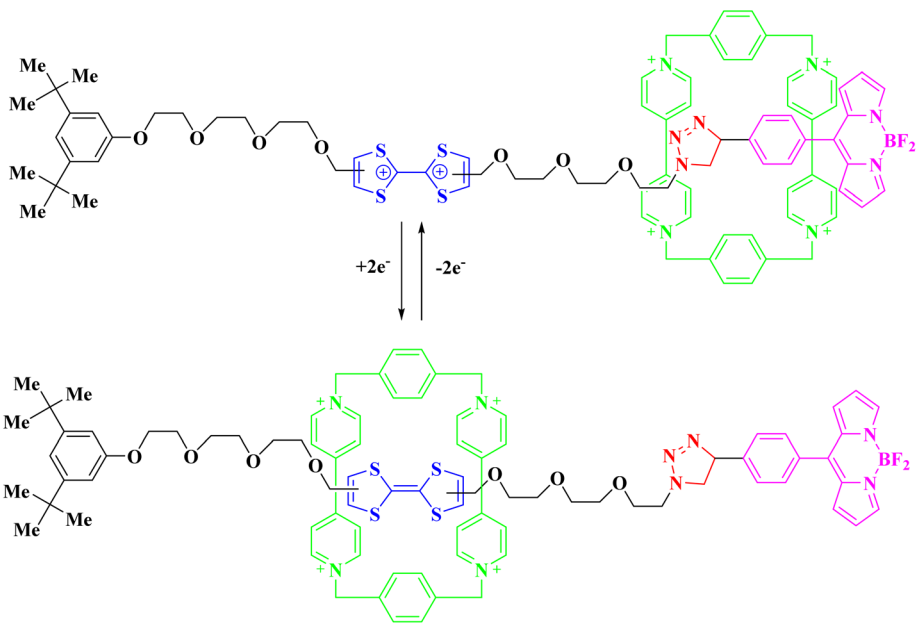

Fig. 6 Redox actuation of a bistable BODIPY rotor [2]. Reproduced with permission from ref. 53, Copyright 2020, American Chemical Society.

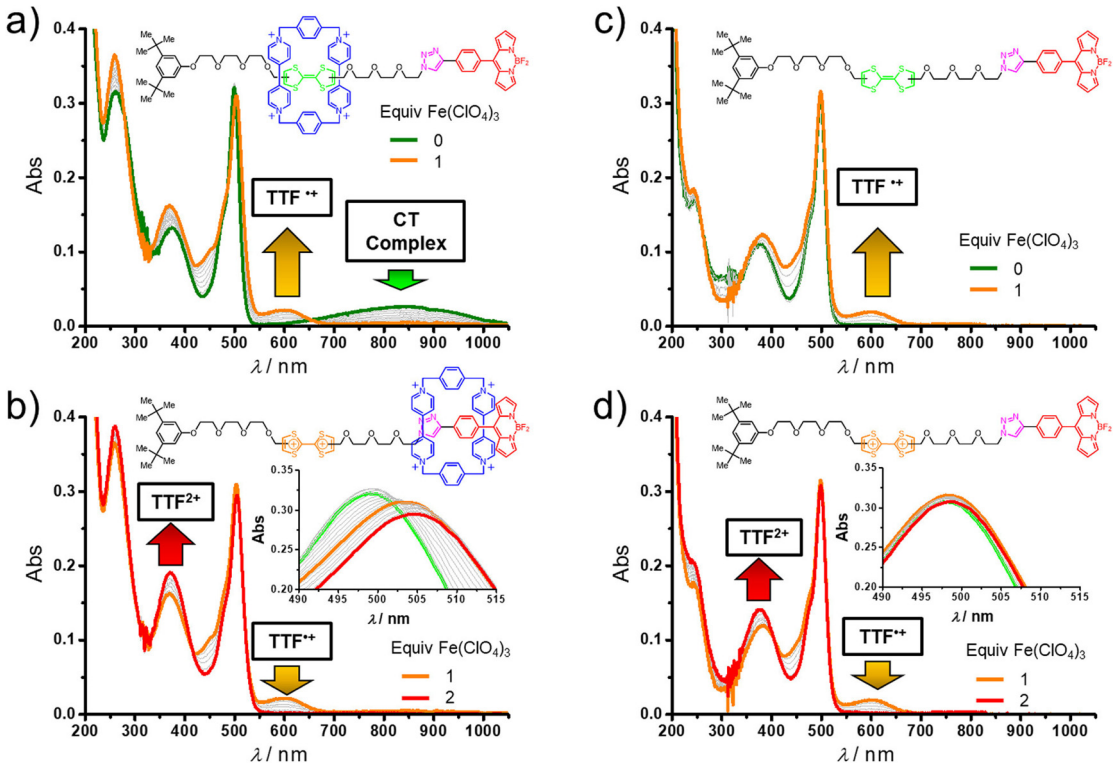

Fig. 7 UV/Vis absorption spectra of Stoddart bistable BODIPY rotor [2]. Reproduced with permission from ref. 53, Copyright 2020, American Chemical Society.

(A) to hop across the AB and DNP units (Fig. 10a). Furthermore, the redox state of the TTF unit within R1E may be switched between its dicationic and neutral forms by sequentially adding oxidising and reducing chemicals without exposure to light. The other $CBPQT^{4+}$ wheel was propelled by this manipulation to alternate between the TTF and DNP units. In order to better understand the redox-driven shuttling of the $CBPQT^{4+}$(B) wheel in R1, extensive UV-vis absorption and ^1H NMR spectroscopic investigations were used to assess the orthogonal controllability of the $CBPQT^{4+}$ wheel shuttling process of R1. The greatly elevated absorption broad band at 540 nm indicates that the neutral TTF unit might be oxidized to a positively charged dicationic TTF^{2+} unit when the oxidizing agent was added to the PSSE (>525 nm) mixed solution of R1 (Fig. 10b). The CT band of the TTF⊂$CBPQT^{4+}$(B) complex at 810 nm completely vanished upon oxidation, indicating that the production of TTF^{2+} may cause the initial TTF-encapsulated $CBPQT^{4+}$(B) wheel to shift to the middle DNP unit, resulting in production of the [3]rotaxane $R1E^{10+}$, in which the $CBPQT^{4+}$ wheels encapsulates both the E-AB and DNP units. The transition from $R1E^{8+}$ to $R1E^{10+}$ caused by oxidation was also confirmed by the recorded ^1H NMR spectra.

Stimuli triggered guest binding/release

The complex synthetic methods used by MIMs, such as active/passive metal template,[99–101] stacking interaction,[85,102,103] halogen/hydrogen bonding,[104,105] or other hydrophobic interactions,[106–108] have also come to light. Functional metal templates and donor–acceptor techniques have been appropriately advanced in this area over the past few years by Leigh *et al.*,[99,109,110] Goldup *et al.*,[101,111,112] Stoddart *et al.*,[113–115] and others.[59,116–121] Tetrathiafulvalene (TTF), 1,5-dioxynaphthalene (DNP), bipyridine, pyridine, viologen, cyclobis-paraquat-*p*-phenylene ($CBPQT^{4+}$), and crown ether derivatives (Fig. 11) are exemplary examples of unique ligands that are preferred critical elements in these systems and aid in developing the dynamic features in the interlocked structures.[69,122–125]

Nandi *et al.* reported a metal templated synthesis of redox-active rotaxane (Fig. 12).[59] By using PhenMC's phenanthroline motif, which has anion binding capabilities as demonstrated by NMR titration and electrochemical techniques. They reported the active metal binding synthesis of RTXN1, a novel redox-active rotaxane. Further, a "π–π" stacking interaction between Phen MC and an alkyne-terminated axle having viologen was used to synthesize RTXN2 rotaxane with multiple redox centers.

Stimuli induced controlled conformation changes

Rotaxanes, a significant class of MIMs, have become crucial contenders for building artificial molecular machines as well

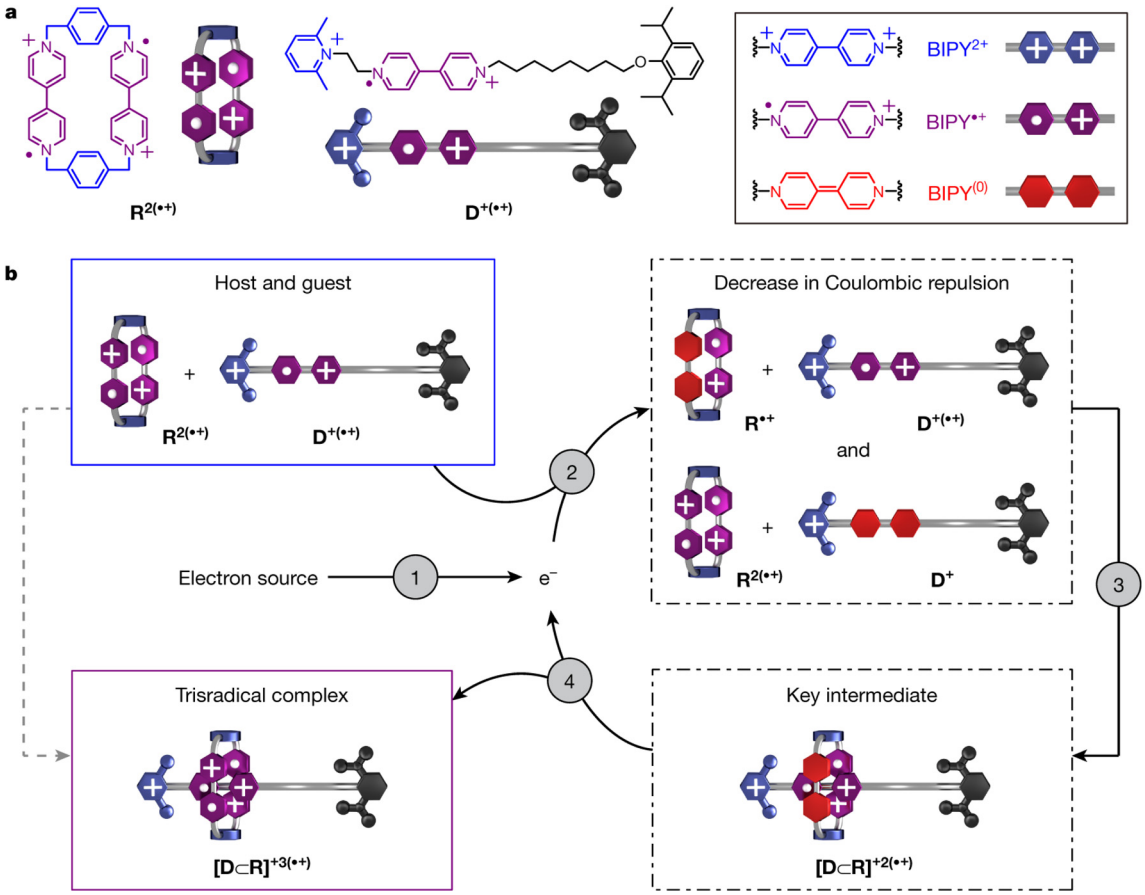

Fig. 8 (a) Structure of the host–guest system consisting of a macrocyclic host and a dumbbell-shaped guest. Each BIPY unit in the system has three redox states, dicationic, radical cationic state and neutral state mentioned in different colors. The variable redox states of viologen is responsible for electron catalysis. (b) The conceptual system for molecular recognition process aided by electrons. The first step involves injecting an electron, second step involves the reduction of one $BIPY^{\bullet+}$ unit in $R^{2(\bullet+)}$ or one $BIPY^{\bullet+}$ unit in $D^{+(\bullet+)}$ to a radical state. Third step involves the quick creation of a crucial intermediate, a $[D\subset R]^{+2(\bullet+)}$ bisradical complex, which is promoted by a reduction in the coulombic repulsion involving the host and guest molecules and the last step involves the oxidation of $[D\subset R]^{+2(\bullet+)}$ bisradical complex by release of an electron to complete the catalytic cycle and resulting in a $[D\subset R]^{+3(\bullet+)}$ trisradical complex as the end product. Reproduced with permission from ref. 97, Copyright 2022, Springer Nature.

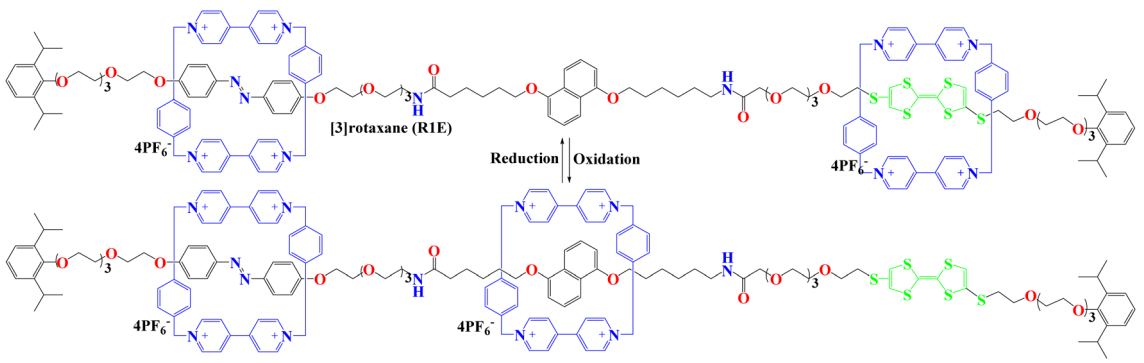

Fig. 9 Gu *et al.*, redox triggered tristable [3]rotaxane(R1). Reproduced with permission from ref. 98, Copyright 2023, Royal Society of Chemistry.

as electronic devices because of their switching and shuttling characteristics.[79,126,127] In response to external stimuli, the macrocyclic component of rotaxane can alter conformation around the axle component.[128–130]

Dumartin *et al.* reported a branched "tail" of the molecular shuttle which is connected to electrochemical hysteresis that opens and closes like a zipper.[131] The MS^{n+} cyclophane is shuttled between two recognition sites in this ring-to-ring

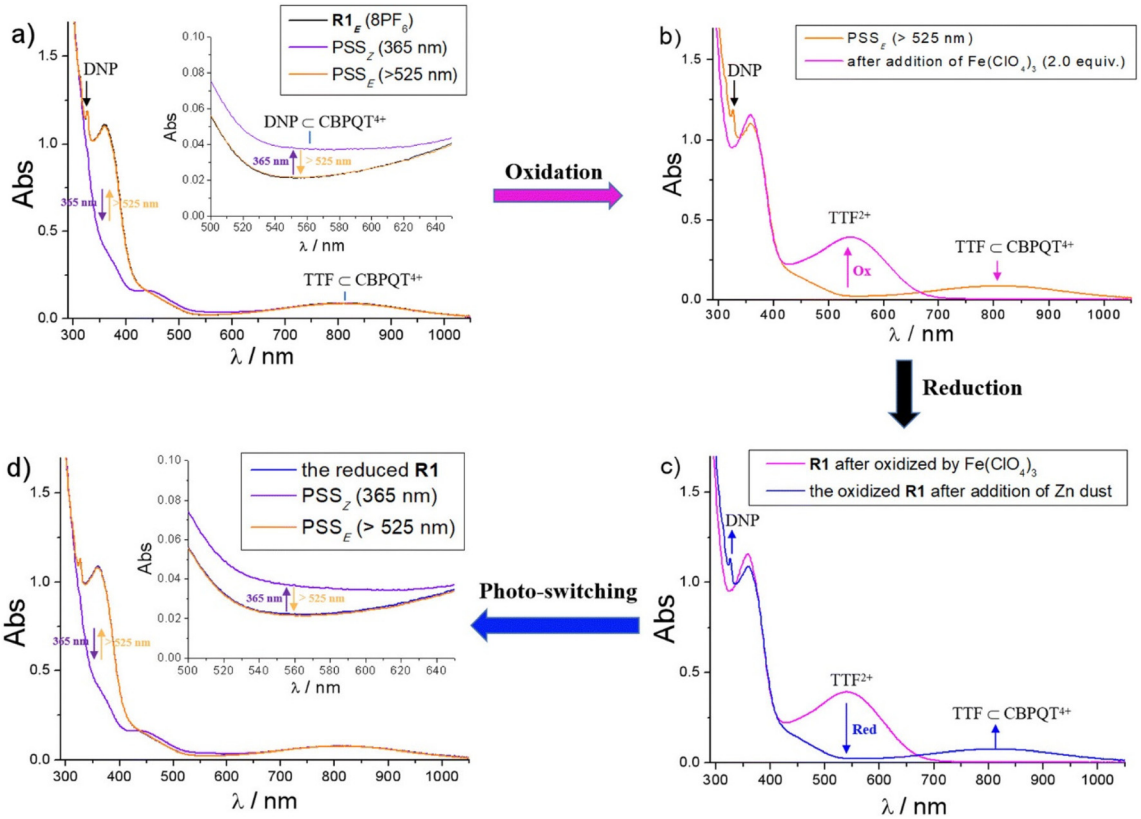

Fig. 10 UV/Vis absorption spectra of Gu *et al.*, tristable [3]rotaxane (R1). Reproduced with permission from ref. 98, Copyright 2023, Royal Society of Chemistry.

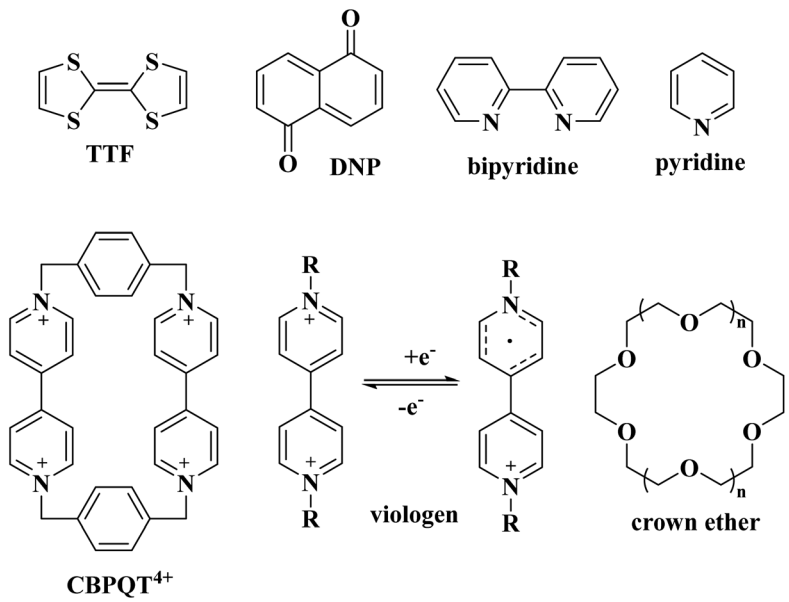

Fig. 11 Redox-active units responsible for switching.

based [2]rotaxane, where one recognition site (Zip-$R^{4(+\bullet)}$) stabilizes *via* radical-pairing in the reduced state. Conversely, donor/acceptor interactions maintain Zip-R^{8+} in its oxidized state as an alternative (Fig. 13).

Methods such as UV-Vis-NIR and ^{1}H NMR spectroscopy were used to investigate the interconversion of Zip-R^{8+} and Zip-$R^{4(+\bullet)}$. Zinc dust was used to reduce Zip-R^{8+} in acetonitrile (MeCN), producing Zip-$R^{4(+\bullet)}$ which has a distinctive near-

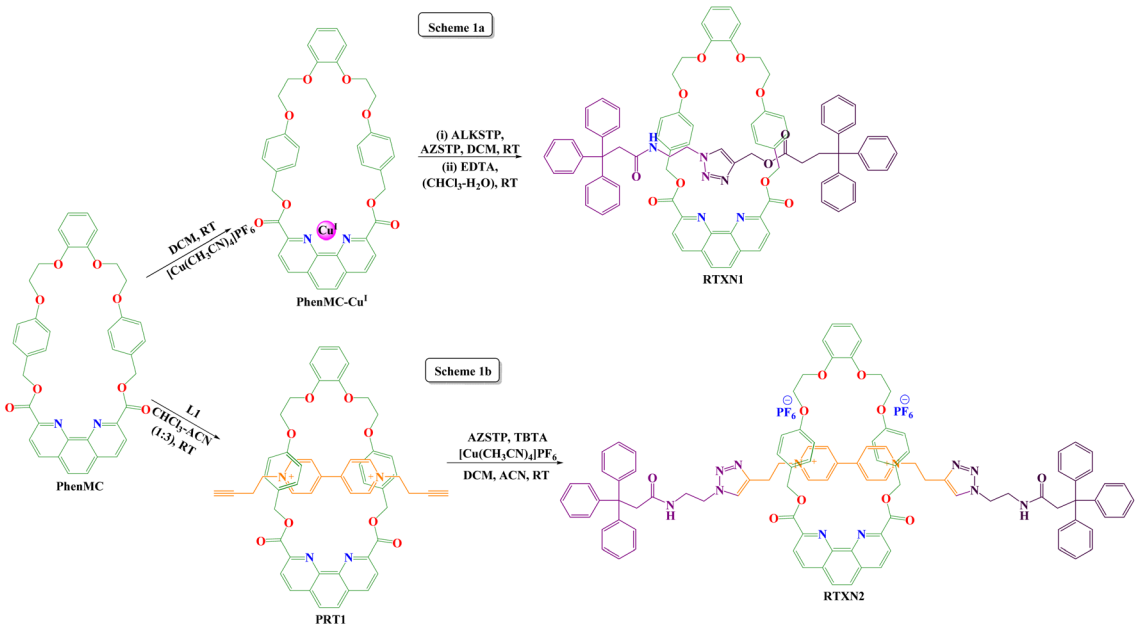

Fig. 12 Nandi's redox-active rotaxane (reproduced with permission from ref. 59, Copyright 2020, Wiley VCH).

infrared (NIR) band with a centre wavelength of 958 nm that confirms the existence of bipyridinium radical-pairing. Two oxidation waves are seen when Zip-$R^{4(+\bullet)}$ was oxidised to Zip-R^{8+} at 100 mV s^{-1} scan rate, demonstrating the existence of slow dynamic processes (Fig. 14). The redox behaviour of the dumbbell component displays a distinct reversible redox wave across a range of scan rates, demonstrating its stability. In contrast, the dynamics of the mechanically interlinked parts impact how the oxidation peaks in Zip-R^{8+} divide. Regardless of the scan rate, Zip-R^{8+} exhibits a distinct reduction wave which becomes broader and shifts to more negative potentials as the scan rate increases. Lower scan rate result in a sharper, more positive reduction wave, which indicates that the radical state has stabilized during the creation of the ring-in-ring recognition motif. The reduction process starts with the innermost cyclophane, leading to the intermediary Zip-$R^{(6+)(2\bullet)}$D.

In Zip-$R^{(6+)(2\bullet)}$D, MS^{4+} is in an electron-rich environment that stabilizes its reduction while requiring more negative potentials than free cyclophane. Moreover, the reduction wave shifts in favour of positive potentials at slower scan rates as they instantly transition into the more stable Zip-$R^{4(+\bullet)}$A state. Due to the restricted interaction between the Zip-$R^{(6+)(2\bullet)}$D and Zip-$R^{4(+\bullet)}$D cyclophanes, rapid scan rates result in a more negative and significant reduction wave, which corresponds to the thorough decrease of the metastable co-conformation of Zip-$R^{4(+\bullet)}$D. At intermediate scan rates, two distinct oxidation waves can be seen. As the scan rate increases, the first obvious oxidation wave at −0.55 V becomes less prominent; nevertheless, at scan rates lower than 1000 mV s^{-1}, another oxidation wave at a more negative potential (−0.65 V) becomes dominant. At lower scan speeds, the more positive oxidation wave is associated with the electronically stabilised fully developed ground-state co-conformationZip-$R^{4(+\bullet)}$A. Further, the metastable co-conformation Zip-$R^{4(+\bullet)}$D, which is capable of swiftly transitioning into the ground-state co-conformation, is reached by the negative oxidation wave. At slow scan rates, the transformation between Zip-R^{8+} and Zip-$R^{4(+\bullet)}$ can be observed as quasi-reversible.

Recently, a novel type of rotaxane known as daisy chain rotaxane has gained significant attention for its role in developing molecular machines. "Daisy chain rotaxanes" refers to a specific type of rotaxane structure where several macrocycles are threaded onto a single axle, akin to a daisy chain. Each macrocycle is linked to the next in a linear arrangement, resembling the petals of a daisy connected in a chain.[132] These structures are of interest to supramolecular chemistry and nanotechnology owing to their special characteristics and potential applications in molecular machines, materials, and drug delivery systems.[133,134] In 2023, Stoddart and colleagues published findings on the template-directed synthesis of redox-active [c3]daisy chain rotaxanes. They describe the design (depicted in Fig. 15A) and synthesis of two such rotaxanes, named [c3]DC2·$18PF^{6-}$ and [c3]DC12·$18PF_6$, employing a combination of radical and anion templation. The arrangement of the self-complementary monomers, along with templation by PF^{6-} counterions, has resulted in the highly efficient formation of [c3]DC2·$18PF^{6-}$ and [c3]DC12·$18PF^{6-}$ with yields approaching full conversion. The mechanically interlinked structure and self-aggregation of [c3]$DC12^{9(\bullet+)}$—a nonaradical nonacationic variant—exhibit significantly improved air stability. Additionally, by employing an electrochemical stimulus, the geometry of the macrocycle, which is formed from [c3]$DC12^{18+}$ in solution, can be easily and reversibly changed between its reduced trisarm-shaped [c3]$DC12^{9(\bullet+)}$ and oxidized cyclic [c3]$DC12^{18+}$ states (Fig. 15B).

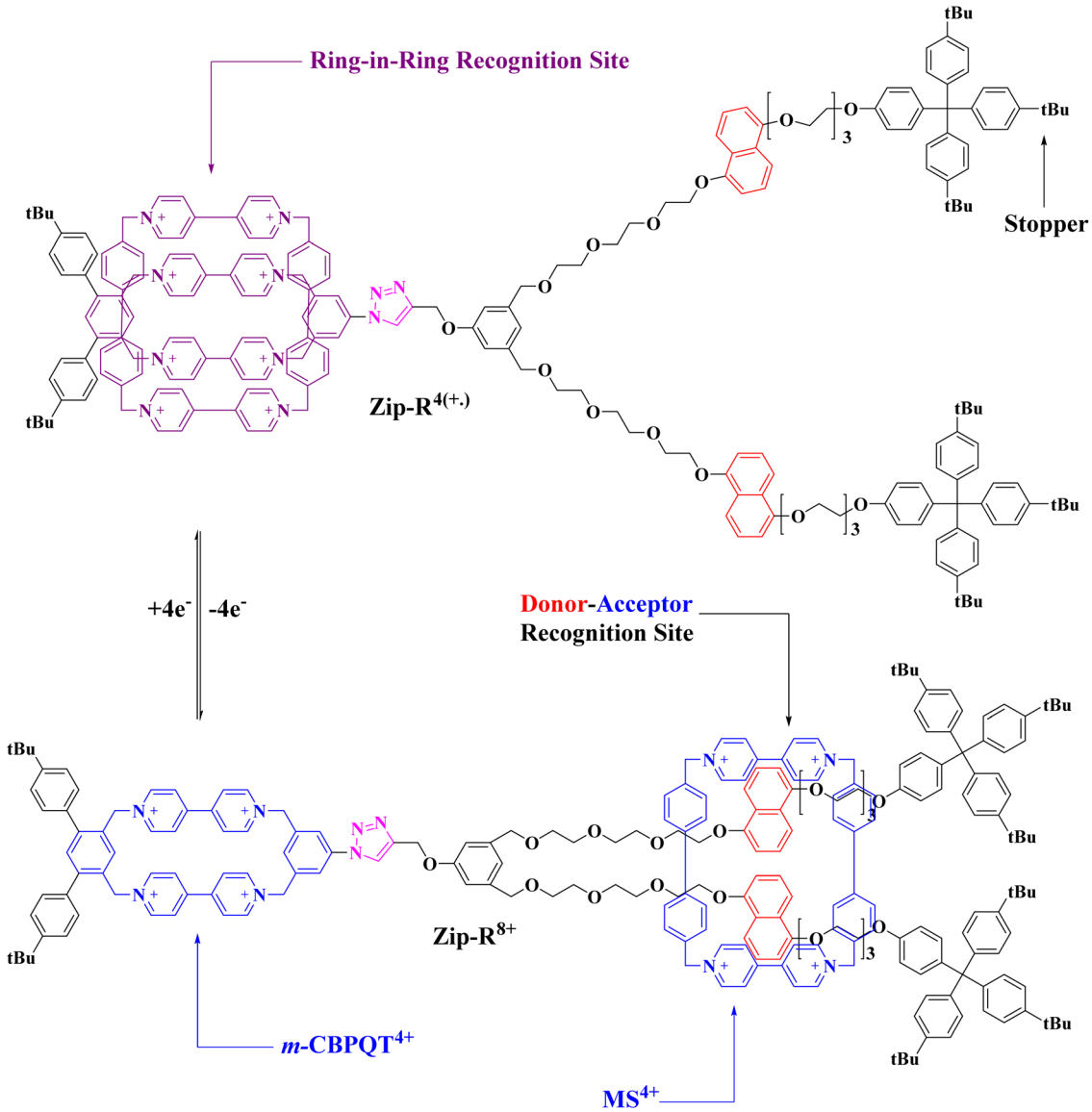

Fig. 13 Dumartin's zipper – [2]rotaxane switching: electrochemically driven actuation of the molecular zipper (Zip-$R^{4(+\cdot)}$/Zip-R^{8+}). (Reproduced with permission from ref. 131, Copyright 2019, American Chemical Society).

^{1}H NMR spectroscopy reveals that the mCBPQT^{4+} rings within [c3]DC12·18PF_6 encircle the triazoles near the stoppers, forming a macrocycle-like co-conformation (Fig. 16b). The solution of [c3]DC12^{18+} turns from colorless to deep purple after reduction with Zn dust in MeCN and a distinctive absorption at 1070 nm is visible in the Vis/NIR spectrum. According to these findings, [c3]DC12^{18+} is reduced to [c3]DC12$^{9(\cdot+)}$, a nonaradical nonacationic state, and the mCBPQT$^{2(\cdot+)}$ rings are moving to interact with the in-chain BIPY$^{\cdot+}$ units (Fig. 16c). The ^{1}H NMR spectrum of [c3]DC12$^{9(\cdot+)}$ indicates that the protons on the nine BIPY$^{\cdot+}$ units and near the BIPY$^{\cdot+}$ units are affected by the paramagnetic properties of the BIPY$^{\cdot+}$ radicals. However, because of their distance from the BIPY$^{\cdot+}$ radicals protons on the stoppers, triazoles, and portions of the oligomethylene chains remain detectable. Thus, the ^{1}H NMR spectrum confirms the positioning of the mCBPQT$^{4(\cdot+)}$ rings on the BIPY$^{\cdot+}$ units, supporting the three-arm star-shaped geometry of [c3]DC12$^{9(\cdot+)}$. Compared to chemical redox processes, electrochemical stimulation provides a cleaner and more convenient way to move across cyclic and trisarm-shaped states. Their Vis/NIR spectra show that when different potentials are applied to a MeCN solution of [c3]DC12·18PF_6 using controlled potential electrolysis (CPE), the solution's color reversibly switches between colorless and deep purple, indicating the presence of [c3]DC12^{18+} and [c3]DC12$^{9(\cdot+)}$, respectively. Demonstrates good chemical stability of the [c3]DC system is demonstrated by the CPE switching process as evidenced by repeated cycles with no discernible alterations in the Vis/NIR spectra (Fig. 16d).

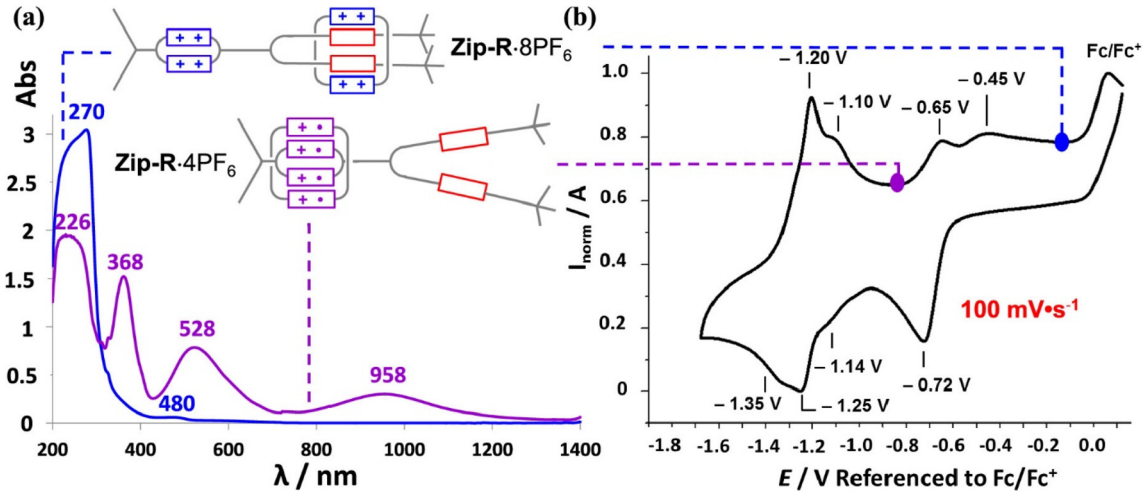

Fig. 14 (a) UV–vis–NIR spectra and (b) CV of the Zip-R·8PF_6 (0.035 and 0.03 mM in MeCN and 0.1 M tetrabutylammonium hexafluorophosphate/MeCN respectively) at RT. (Reproduced with permission from ref. 131, Copyright 2019, American Chemical Society).

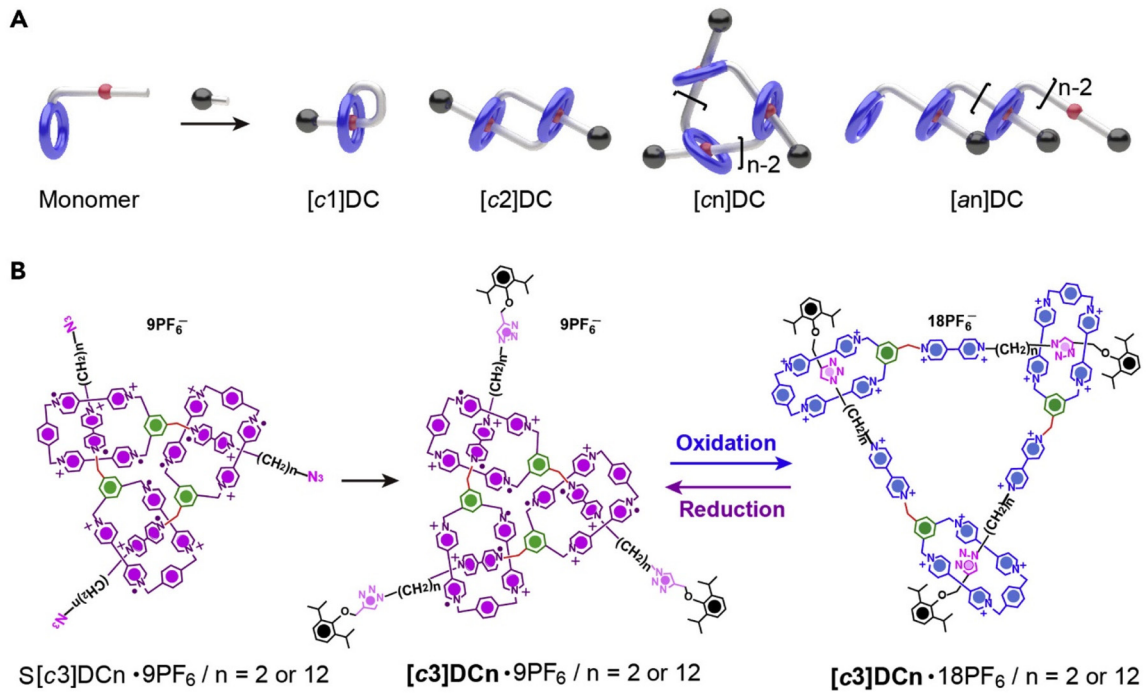

Fig. 15 Stoddart's redox switchable [c3]daisy chain rotaxanes. Reproduced with permission from ref. 135, Copyright 2021, Elsevier.

Kinetics of rotaxane redox switching

Rotaxane macrocycle can go amid several stations built in a dumbbell 'track'. An external stimulus must be given to initiate this shuttling process, given that it alters the stations' based on the affinities and provides the macrocycle with a push to move and produce a newly stable translational isomer. Controlling the kinetics of the system is crucial for effectively utilizing this motion.

Andersen *et al.* reported the kinetics of switching of $CBPQT^{4+}$ by changing ionic environment of rotaxane from central TTF unit to peripheral oxyphenylene unit of macrocycle.[136] UV-Vis-NIR were used to investigate the kinetics of electrochemical switching of $CBPQT^{4+}$. Initially the macrocycle ($4PF_6$) mainly exists in the "unswitched" form, where $CBPQT^{4+}$ surrounds the central TTF station (Fig. 17). Introducing a one equivalent of $Fe(ClO_4)_3$ allows for investigating the switching process's kinetics in the oxidized [2]rotaxane, where $CBPQT^{4+}$ moves between the stations. The presence of 0.1 M $Fe(ClO_4)_3$ solution significantly enhances the rate constant in connection with the switching process as compared to the absence of the salt. Moreover, the TTF unit's oxidation rate displayed a signifi-

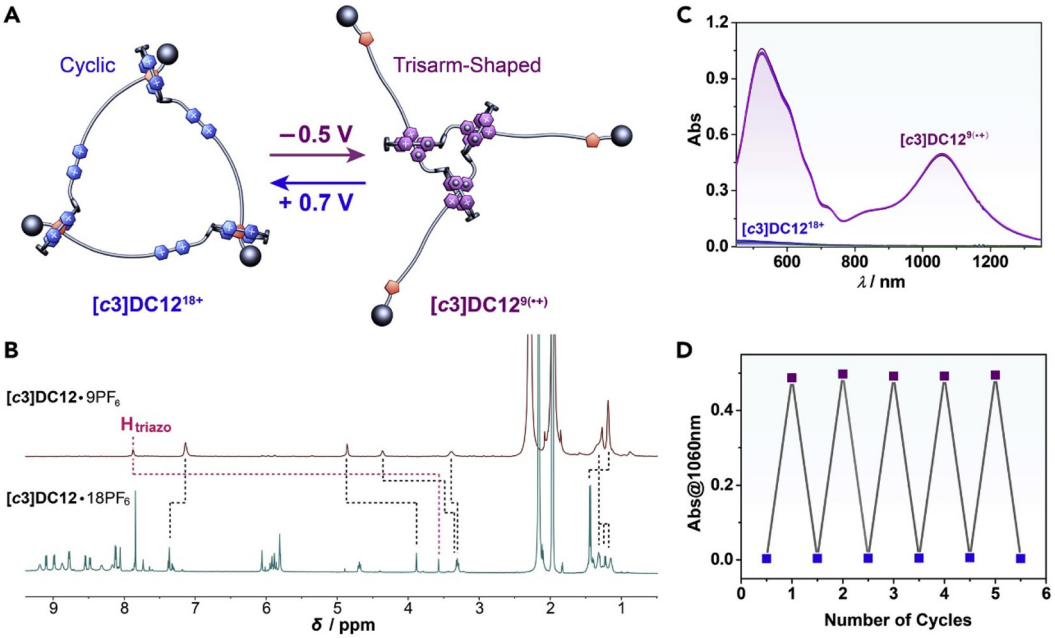

Fig. 16 (A) Electrochemical switching between [c3]DC12^{18+} and [c3]DC12$^{9(\bullet+)}$. (B) ^{1}H NMR spectra, (C) Vis/NIR absorption spectra, (D) reversible switching cycle. Reproduced with permission from ref. 135, Copyright 2021, Elsevier.

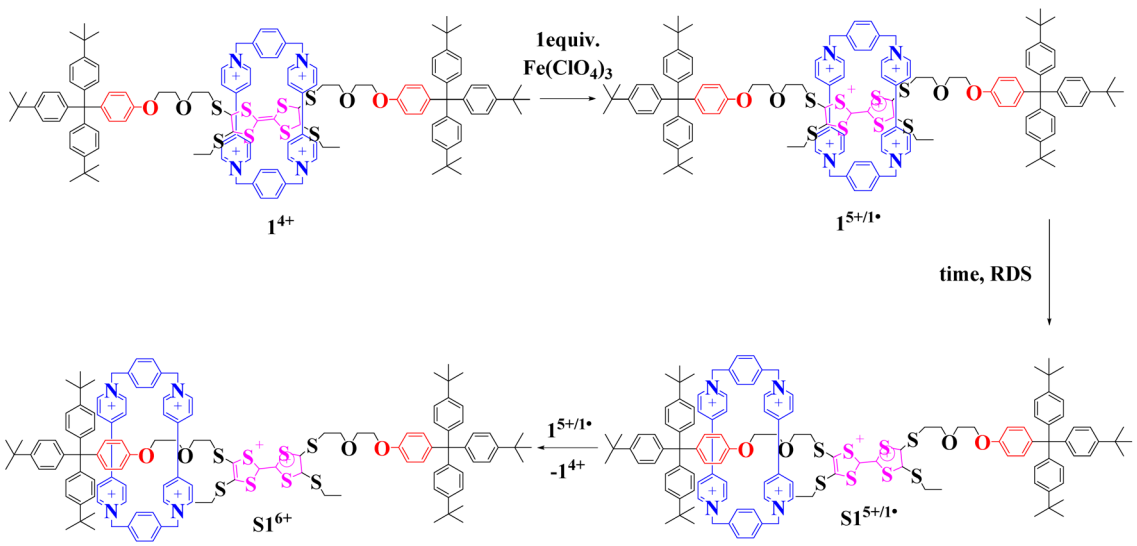

Fig. 17 Effect of adding $Fe(ClO_4)_3$ salt while shuttling of rotaxane. The mono-oxidised rotaxane $1^{5+/1\bullet}$ is produced first. Second, switching $1^{5+/1\bullet}$ produces the switched form of [2]rotaxane $S1^{5+/1\bullet}$, which disproportionately produces the initial, ground state rotaxane 1^{4+} and the doubly-oxidised switched molecule $S1^{6+}$. RDS = rate determining step (reproduced with permission from ref. 136, Copyright 2019, Royal Society of Chemistry).

cant increase. Different PF_6^- salts with varying ammonium cations (n-Bu_4N^+, Et_4N^+, Me_4N^+, and NH_4^+) amplified the switching rate by the order of 1.5 to 1.8.

The most pronounced enhancement was observed with the most significant cation, n-Bu_4N^+. However, the resulting rate constants were closely clustered, indicating that the size of the cation has minimal impact on the kinetics, if any. When comparing n-$Bu_4N{\cdot}PF_6$ to n-$Bu_4N{\cdot}ClO_4$, the rate constant increased significantly when the smaller ClO_4^- anion was used, approximately 3.5-fold higher. These observations are explained by changes in the ion-pair equilibrium caused by the presence of salts, which influence the binding potential of CBPQT^{4+} onto the stations in the dumbbell. Additionally, the salts assist in stabilizing the transition state as CBPQT^{4+} overcomes the significant thioethyl (Set) barrier. Adding salts offers a convenient approach to enhance the transitioning rates in CBPQT^{4+} based electroactive molecular shuttles.

Chemical/redox switching in catenanes

A member of mechanically interlocked molecules (MIMs) known as catenanes is made up of two or more macrocycles (rings) that are woven through one another and are unable to be separated without breaching a covalent interaction. The word "catenane" is derived from the Latin word "*catena*", which means chain, and it refers to their interconnected character.[137] Despite having different topologies, catenanes and rotaxanes can be considered molecular siblings since they can be made from a pseudorotaxane, a supramolecular species in which one or more macrocycles ring a thread.[138] The most stable species in solution are usually produced by noncovalent bonding interactions that induce thermodynamic threading of a linear component through the macrocycle (Fig. 18).[139–142]

As contenders for the development of molecular switches, machines, and memory devices, bistable catenanes represent a family of functional molecules that is very intriguing.[143,144] The propensity of these molecules' parts to undergo specific and reversing large-amplitude motions (of one component with respect to another) without affecting their mechanically interlocked structure makes them appropriate for the fabrication of artificial nanodevices. Numerous reports concerning the chemical, electro/photochemical induced molecular shuttles have been published, and this behavior has been extensively investigated using numerous techniques.[145–147] Catenanes are at the forefront of this field to construct artificial molecular machines and take advantage of the dynamics of interlocked structures in polymers, metal/covalent–organic frameworks (M/COFs), and other materials.[148–152] Their research has resulted in significant advancements that have significance for various scientific fields, from biology to soft matter physics, as well as supramolecular chemistry.[153]

Like rotaxanes, catenanes have a naming system where the term is preceded by square brackets denoting the number of macrocycles that make up a catenane. So a molecule made of n macrocycles is called a [*n*]catenane.[154] (Fig. 11) Catenanes' interlocked design can be functionally utilized in several ways. Catenanes are appealing candidates for use in molecular machines due to the dynamics of the substantial amplitude motions that their components can undergo.[155] A rotary motor can be built based on the 360° rotation of one ring about the other or the change in the relative placement of the rings, which can be utilized as a switch. This characteristic can be exploited to bind substrates precisely because the cavity created by interlocking rings can be employed to hold functional groups in precise places in 3D space.[143,147,156–159]

Mechanism of redox switching in catenanes

The ability of catenane structures to undergo reversible conformational changes or switch between several states in response to a chemical/electrochemical stimulus is called stimuli-responsive switching in catenanes (Fig. 19). This behavior is made possible by including redox-active units in the catenane's macrocycles, which enable electron transfer during the electrochemical reaction.

This electrochemical switching in catenanes can occur in following steps: (1) presence of redox active functional groups in catenanes. Switchable catenanes often contain redox-active groups within their macrocycles, such as metal centers or organic moieties. These redox-active units can undergo revers-

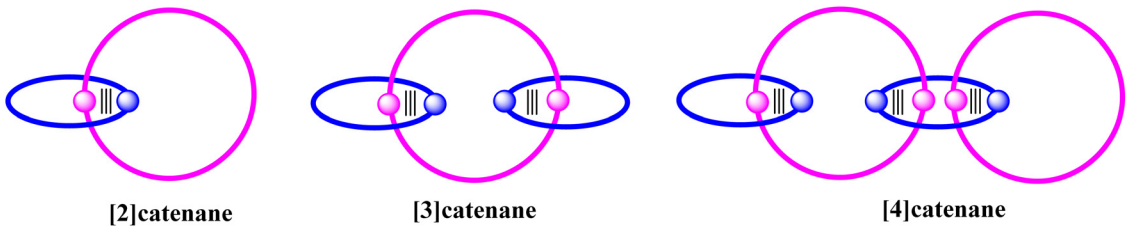

Fig. 18 Cartoon representation of different catenanes.

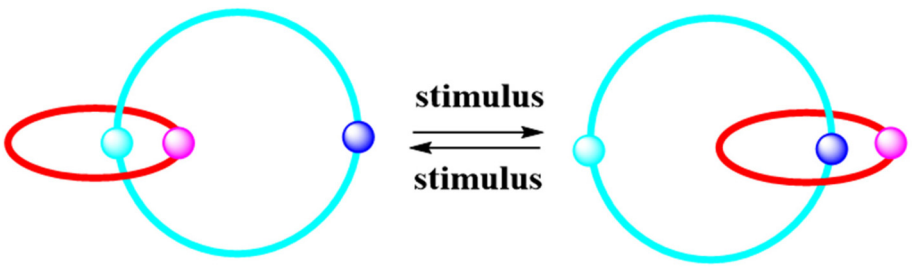

Fig. 19 Cartoon representation of catenane switching in presence of external stimuli.

ible oxidation and reduction reactions chemically or electrochemically, leading to changes in their electronic state and overall conformation of the catenane. (2) Activation of redox groups: an electrical potential is applied to the catenane system (*e.g.*, through cyclic voltammetry or other electrochemical techniques), and the redox-active groups within the macrocycles can accept or donate electrons, depending on the applied potential. This electron transfer process induces a change in the redox state of the catenane, which in turn alters the interactions between the interlocked macrocycles. (3) Changes in the redox state of the catenane can cause conformational switching, which causes the threaded macrocycles to move about one another. Depending on the design of the catenane and the specific redox-active groups, this movement may involve switching between different binding sites or adopting different spatial arrangements. (4) Reversibility of catenanes: electrochemical switching in catenanes is typically reversible. Once the electrical potential is removed or changed, the redox-active groups can undergo the reverse electron transfer process, leading the catenane to return to its initial state or adopt a different conformation. In cases, where the switching is carried out chemically using oxidant or reductant, the reverse reaction can bring down the catenane to its original state.

Due to the possibility of using redox-switchable catenanes in molecular machines, sensors, and other responsive nanoscale systems, they have attracted a lot of attention. The ability to control their conformation and properties through chemical/electrochemical stimuli opens up new possibilities for dynamic and adaptive materials at the molecular level. However, it's essential to note that the design and specific behavior of redox-switchable catenanes can vary significantly depending on the choice of redox-active groups and the overall structure of the interlocked molecules.

Recent catenanes redox/electrochemical switches and their different applications

Switching between binding sites

Catenanes with multiple binding sites can exhibit redox-chemical switching between different binding states. By controlling the redox potential, the catenane can be switched between states where specific sites are accessible or blocked, affecting its binding properties. The ability of these interconnected molecules to exhibit reversible conformational changes in response to variations in the oxidation state of redox-active units within the catenane structure is referred to as "redox-driven conformational switching" in catenanes.[153] Redox-active groups, which can accept or donate electrons, are included in the catenane's macrocycles to facilitate this behavior. Recently, Stoddart and co-workers demonstrated an artificial molecular rotor made of [3]catenane and 2 cyclobis(paraquat-*p*-phenylene) ($CBPQT^{4+}$) rings that rotate in a single direction around a 50-membered loop while being impacted by an electric field in solution[122] (Fig. 20a). The two rings' single-directional circumrotation during this switching does not necessitate the breakage of any covalent bonds. It takes only a few minutes to complete two redox cycles that need the single-directional circumrotation of both the tiny rings across 360° about the loop (Fig. 20b). In an oxidizing environment, the two $CBPQT^{4+}$ rings surround the loop. One of the rings occupy the well formed by the BPM unit, necessitating the other ring to cross the IPP unit. Two mechanically interlocked $CBPQT^{4+}/^{2(+\bullet)}$ rings, a switchable barrier connected to the PY^{+} unit, two switchable viologen ($V^{2+}/^{+\bullet}$) recognition sites, and a steric hindrance (IPP) are essential for the production of unidirectional motion (Fig. 20c) of the two rings with regard to the loop. The BPM unit is surrounded by $[CBPQT\text{-}B]^{4+}$ because of repulsive coulombic forces, whereas the T unit is originally surrounded by $[CBPQT\text{-}A]^{4+}$. Reduction occurs when six electrons are added to the [3]catenane (Fig. 20c, step 1), changing the $CBPQT^{4+}$ rings into $CBPQT^{2(+\bullet)}$ and the V^{2+} units to $V^{+\bullet}$. An increase in attractive radical–radical interactions is accompanied by a decrease in coulombic interactions (Fig. 20c, II). On the other hand, for a $CBPQT^{2(+\bullet)}$ ring, the barrier to cross the IPP unit is significantly greater than the barrier to cross the PY^{+} unit. Therefore, $[CBPQT\text{-}A]^{2(+\bullet)}$ traverses the PY^{+} unit before continuing clockwise to $V^{+\bullet}$, and $[CBPQT\text{-}B]^{2(+\bullet)}$ moves concurrently to occupy the $V^{+\bullet}$ unit that is adjacent to the IPP unit. The stable $[3]CMM^{7+6\bullet}$ form in this overall reduced state is the one in which the $V^{+\bullet}$ binding sites are encircled by both $CBPQT^{2(+\bullet)}$ rings. The $[CBPQT\text{-}A]^{4+}$ ring is installed on the BPM unit and the $[CBPQT\text{-}B]^{4+}$ ring is installed on the T unit by a biased Brownian motion (Fig. 20c, III) that results from further oxidation (Fig. 20c, step 2). Overall, a single redox cycle initiates the 180° unidirectional rotation and positional exchange (Fig. 20c, I′) amongst the two $CBPQT^{4+}$ rings. The rings complete a 360° clockwise circumrotation across the loop and return to their original starting places after a second redox cycle (Fig. 20c, steps 3 and 4). It takes only a few minutes to complete two redox cycles for the two tiny rings to circumrotate 360° in relation to the loop in a unidirectional manner. Additionally, by chemically modifying one of the two tiny rings, the co-constitution of the [3]catenane permits adherence to the electrode surface, facilitating spatially directed rotation for a fixed frame of reference and the conversion of electrical energy into mechanical energy at a surface. On the other hand, redox control of the two-dimensional potential energy landscape of [3]catenane drives the energy ratchet mechanism of electric molecular motors. The design of the loop fundamentally modifies the energy landscape in a way that allows the redox potential to oscillate externally, providing the energy required to achieve unidirectionality and harness the molecular system's Brownian motion.

Because of its complex synthetic process and the few interactions, such as van der Waals forces among the cycloalkane as well as the ring, which lead to the statistical synthesis of catenanes during the cyclization stage, switching in higher catenanes is always tricky.[160] A recent example was provided by Stoddart and coworkers, who reported the successful synthesis

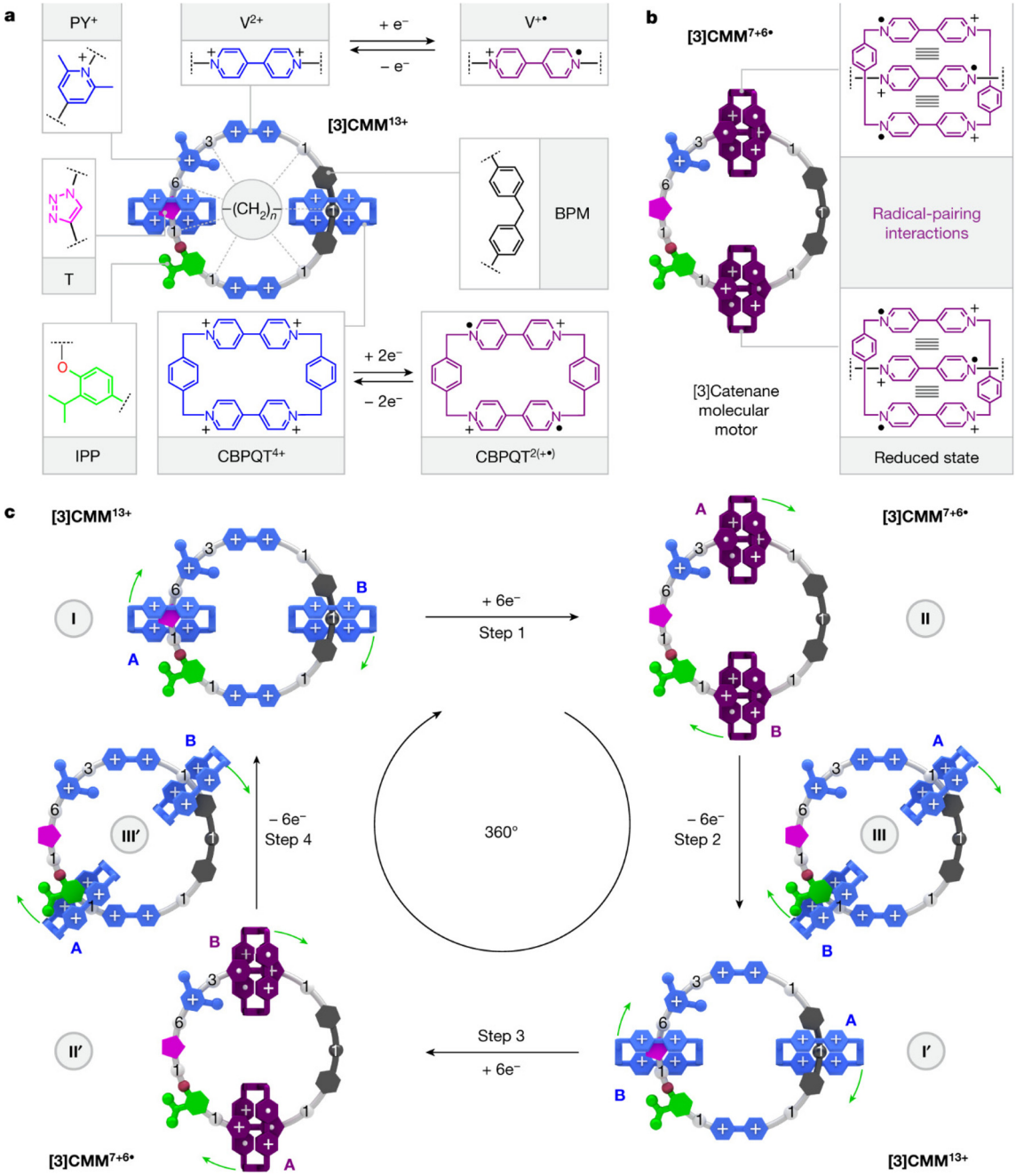

Fig. 20 (a) Graphical depictions of the oxidised state of the [3]catenane molecular motor [3]CMM^{13+}, together with important structural components. The terms CBPQT^{4+}, CBPQT$^{2(+\cdot)}$, V^{2+}, $V^{+\cdot}$, BPM, IPP, T, and PY^{+} refer to the cyclobis (paraquat-*p*-phenylene) rings, the bisradical dicationic states of cyclobis (paraquat-*p*-phenylene), the viologens, the radical cationic states of the viologens, the bis(4-methylenephenyl)methane, the isopropylphenylene, the triazole, and the 2,6-dimethypyridinium units, respectively, (b) graphical depictions of the reduced state of the [3]catenane molecular motor [3]CMM$^{7+6\cdot}$, CBPQT$^{2(+\cdot)}$ rings and the $V^{+\cdot}$ units interact through radical-pairing, (c) redox operation of [3]CMM$^{13+/7+6\cdot}$. Reproduced with permission from ref. 122, Copyright 2023, Springer Nature.

of two catenanes: a tetracosacationic radial [5]catenane, which comprises four mechanically interlocked 4^{+} charged rings around an 8^{+} charged ring and can contain up to 24 positive charges, and a dodecacationic [3]catenane, which is consisting of three mechanically interlocked 4^{+} charged rings regardless of their common coulombic attraction (Fig. 21).[161]

Template-directed methods are typically required for mechanical bond formation to reconcile the entropy loss from the interlocking of mechanical bonds and the enthalpic gains from the molecular templation. However, under reducing conditions to a fundamentally based template negated during oxidation, [*n*]catenanes are formed, both are enthalpically and

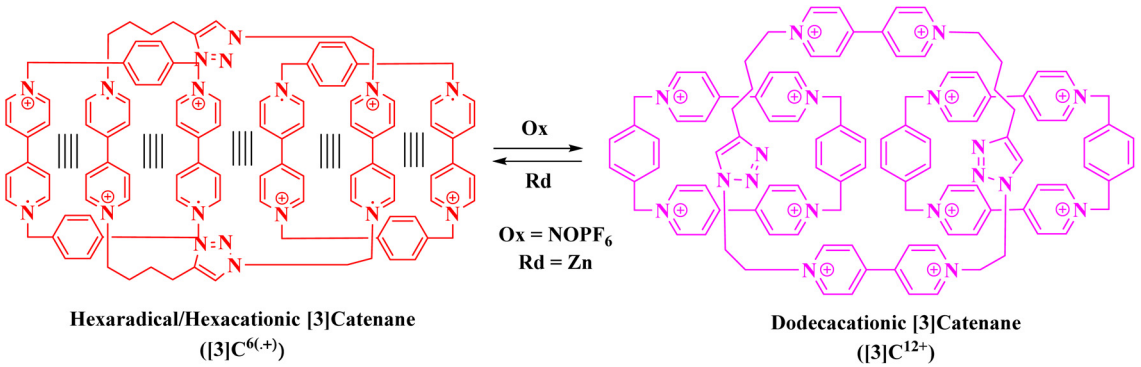

Fig. 21 Stoddart's dodecationic [3]catenane (reproduced with permission from ref. 161, Copyright 2018, Elsevier).

entropically demanding. Additionally, this catenane can switch chemically or electrochemically into two stable states: dodecacationic as well as hexaradical hexacationic. These two redox states, which were demonstrated to have two distinct geometries in their solid states by X-ray diffraction, enabled for the formation of excellent single crystals. The two exterior cyclophanes' circumrotation from surrounding the triazole linkers to include the $BIPY^{(\bullet+)}$ units after being reduced from $CBPQT^{4+}$ to $CBPQT^{2(\bullet+)}$ led to these geometries. As evidenced by CV and UV-vis-NIR spectroscopy, the molecular switch is reversible in action and can be switched for a minimum of five times in solution (Fig. 22b and c).

Radical pairing interactions between viologen units in catenanes have played a significant role in synthesizing different derivatives of catenanes. Moreover, sometimes it also acts as a procrastinator in stabilizing the co-conformation derivatives.[162,163] A similar approach has been used by Wang *et al.*, where they reported an oxime condensation product, octa cationic homo-catenane, that possesses redox induced switching (Fig. 23).[164]

The switching behavior was established through UV/Vis/NIR and NMR spectroscopy. In UV/Vis/NIR spectra, they found a broad peak centered at 1100 nm, establishing the presence of $(BIPY^{+\bullet})_2$ after the addition of Zn dust (Fig. 24). This confirms the switching from phenylene units to BIPY units upon reduction. The findings were supported by ^1H NMR, where a broadening of the baseline after adding Zn dust was noted. The [2]catenane is found in an oxidised state in a co-confor-

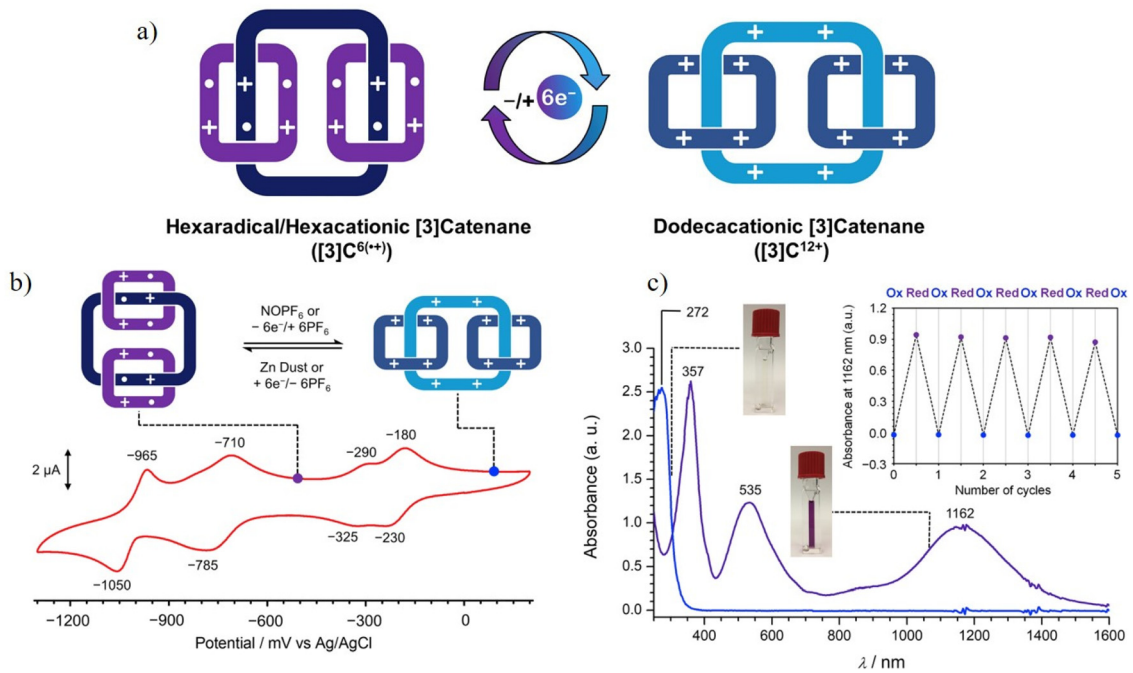

Fig. 22 (a) Stoddart's dodecationic [3]catenane, (b) cyclic voltammogram of [3]C·12PF_6 (0.1 M $TBAPF_6$/MeCN), (c) UV-vis-NIR spectra of $[3]C^{12+}$ (blue) and $[3]C^{6(\bullet+)}$ (purple) are depicted. Insets show absorption intensities of $[3]C^{12+}$ (blue dots) and $[3]C^{6(\bullet+)}$ (purple dots) at 1162 nm wavelength, indicating reversible switching between the two states across five cycles using Zn dust and $NOPF_6$ as reducing and oxidizing agents, accompanied by photographs of the solutions (reproduced with permission from ref. 161, Copyright 2018, Elsevier).

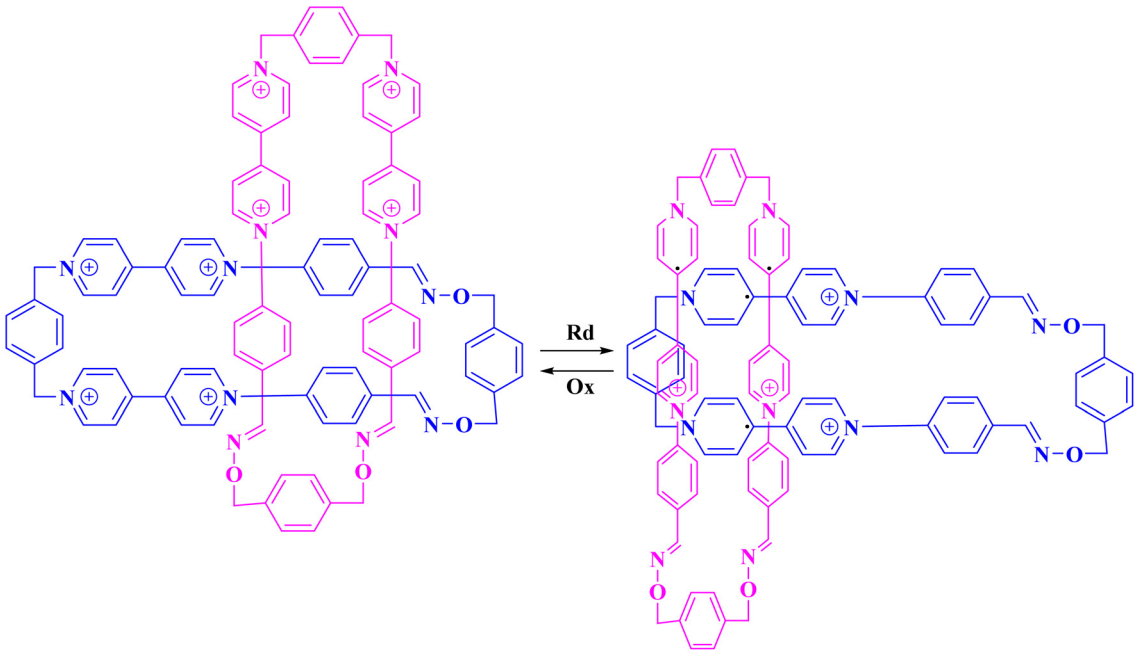

Fig. 23 Wang's Oxime product catenane (reproduced with permission from ref. 164, Copyright 2020, Wiley-VCH).

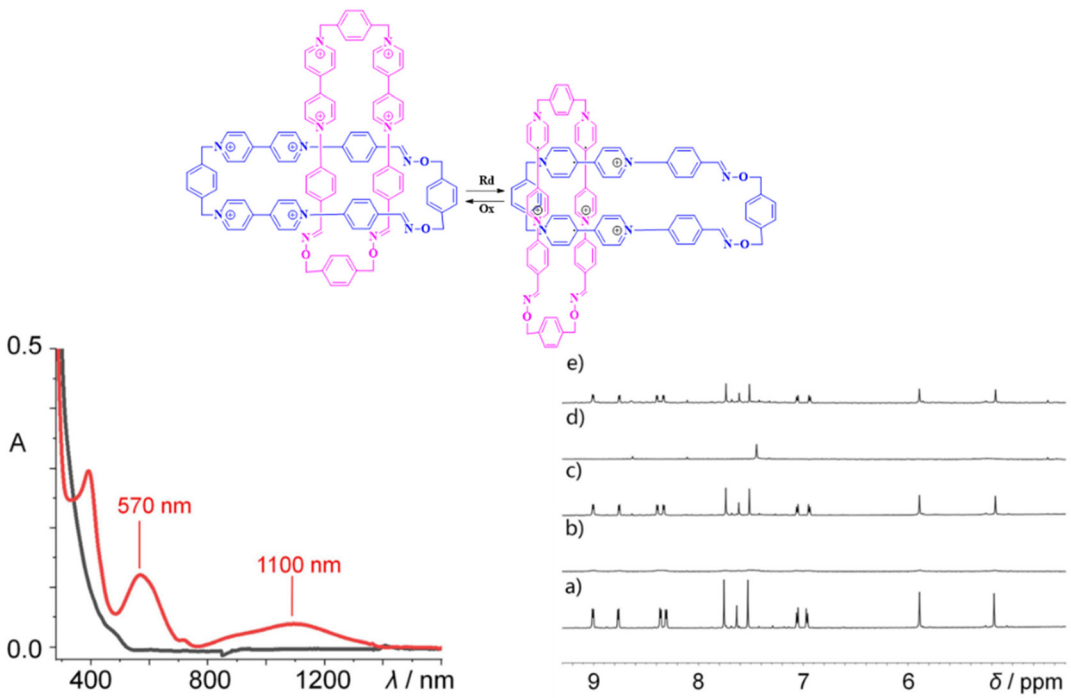

Fig. 24 UV/Vis (left) and ^{1}H NMR spectra (right) Wang's catenane switching (reproduced with permission from ref. 164, Copyright 2020, Wiley-VCH).

mation where one of its two macrocycles encircles a phenyl unit of another, preventing coulombic repulsion between the components of $BIPY^{2+}$. The [2]catenane moves mechanically after reduction, causing another co-formation in which the interactions between its two $BIPY^{+\bullet}$ radical cations have radical pairing interactions.

Conclusion and future prospects

The emergence of a new form of covalent and non-covalent bonding in multifunctional architectures opens the most significant window of opportunity for chemical sciences. This also applies to the mechanical bond. Some of the most complex structures and fascinating synthetic molecular devices have been created because of the chemistry of "small" mechanically linked molecules.[165–169] The use of the mechanical bond in materials research has just recently begun to take off.[170] However, chemists have tried these mechanically interlocked molecules, *i.e.*, rotaxanes and catenanes for applications such as nanomotors, *etc.* where precise molecular level control has been achieved. In its most comprehensive scope of applications, they began to endow such molecules as making molecular machines,[171–174] molecular sensors,[175–179] molecular electronics,[180–183] drug delivery,[184–186] molecular switches,[164,187–189] and, catalysis.[176,190–192]

The molecular switching discussed herein has different binding sites responsible for shuttling/switching when an external stimulus is applied. This review covered recent progress in molecular switching of rotaxanes and catenanes. Herein, we demonstrated how different binding sites in rotaxanes, such as Tetrathiafulvalene (TTF), 1,5-dioxynaphthalene (DNP), bipyridine, pyridine, viologen, and cyclobis-paraquat-*p*-phenylene ($CBPQT^{4+}$), *etc.*, activated in the presence of different external stimuli like, electric current applied, pH change, addition of acid/base, solvent polarity changes, guest induced, or, addition/removal of electrons from these units. On the contrary, catenanes have different binding sites, like $CBPQT^{4+}$, DNP, NDI, BIPY, *etc.*, responsible for switching. These binding sites get activated by external stimuli like reduction/oxidation, pH change, acid/base addition, cation/anion addition, or change in solvent polarity. These switching will further result in co-conformational changes of these mechanically interlocked molecules, and come its initial conformation when stimuli are removed. This reversible conformational change is the procrastinator in comprehending its most comprehensive applications.

Future research on mechanically interlocked molecules may focus on biological, environmental, and medical applications. We believe that there is a need of novel synthetic strategy which reduce the synthetic complexity like reducing multistep synthetic processes, making their preparation labour-intensive and time-consuming and improving yield of product. There is also a need of improving solvent and environment influence such as solvent polarity, temperature, and pH of reaction mixture during the synthesis. However, rotaxanes and catenanes can sometimes be trapped kinetically in one conformation because of energy barriers hindering the transition to other states. Overcoming these barriers to achieve controlled switching is still needed, especially for complex systems that significantly improve its widest applications. In some cases, multiple regioisomers (different positional/region isomers) of rotaxanes and catenanes can be formed during synthesis. These isomers can have various switching properties and stabilities, complicating the isolation and characterization of the desired product can lead to significant applications. On the laboratory scale, significant progress has been accomplished with the design and synthesis of rotaxanes and catenanes. However, larger-scale applications for mechanically interlocked molecules are still a proof of concept. Perhaps, incorporating rotaxanes and catenanes into functional devices or applications can be complex and working on these issues is highly appreciated. Last but not the least, rotaxanes and catenanes form multiple regioisomers (different positional isomers) during synthesis, and these isomers can have other switching properties and stabilities, complicating the isolation and characterization. Despite these difficulties, continued research is concentrated on finding solutions and creating plans to utilize the special switching abilities of rotaxanes and catenanes for various applications.

Conflicts of interest

The authors declare that they have no known competing financial interests or personal relationships that could have appeared to influence the work reported in this paper.

Acknowledgements

The authors thank Director and support staff of CSIR-CECRI for their constant encouragement and support. CECRI manuscript number: CECRI/PESVC/Pubs/2024-024.

References

1 J.-M. Lehn, From matter to life: Chemistry?!, *Resonance*, 1996, **1**, 39–53.
2 V. Jayant, S. Alvi and R. Ali, in *Pharmaceutical Applications of Supramolecules*, ed. N. Goel and N. Kumar, Springer International Publishing, Cham, 2022, pp. 17–53.
3 All Nobel Prizes in Chemistry, **https://www.nobelprize.org/prizes/lists/all-nobel-prizes-in-chemistry**, (accessed 17 June 2023).
4 P. J. Cragg, *Supramolecular Chemistry From Biological Inspiration to Biomedical Applications*, Springer, Dordrecht, Heidelberg, London, New York, 2010.
5 A. G. P. Maloney, P. A. Wood and S. Parsons, Intermolecular interaction energies in transition metal coordination compounds, *CrystEngComm*, 2015, **17**, 9300–9310.
6 G. R. Desiraju, The C–H···O Hydrogen Bond: Structural Implications and Supramolecular Design, *Acc. Chem. Res.*, 1996, **29**, 441–449.
7 Y. Kim, W. Li, S. Shin and M. Lee, Development of Toroidal Nanostructures by Self-Assembly: Rational Designs and Applications, *Acc. Chem. Res.*, 2013, **46**, 2888–2897.

8 F. Diederich and M. Gómez-López, Supramolecular fullerene chemistry, *Chem. Soc. Rev.*, 1999, **28**, 263–277.
9 K. Szalewicz, in *Encyclopedia of Physical Science and Technology (Third Edition)*, ed. R. A. Meyers, Academic Press, New York, 2003, pp. 505–538.
10 *Cell Biology (Third Edition)*, ed. T. D. Pollard, W. C. Earnshaw, J. Lippincott-Schwartz and G. T. Johnson, Elsevier, 2017, pp. 53–62.
11 C. Misra, R. K. Paul, N. Thotakura and K. Raza, in *Nanoparticle Therapeutics*, ed. P. Kesharwani and K. K. Singh, Academic Press, 2022, pp. 293–325.
12 E. Fischer, Einfluss der Configuration auf die Wirkung der Enzyme, *Ber. Dtsch. Chem. Ges.*, 1894, **27**, 2985–2993.
13 W. M. Latimer and W. H. Rodebush, Polarity and Ionization from the Standpoint of the Lewis Theory of Valence, *J. Am. Chem. Soc.*, 1920, **42**, 1419–1433.
14 The Discovery of Crown Ethers (Noble Lecture) – Pedersen – 1988 – Angewandte Chemie International Edition in English – Wiley Online Library, **https://onlinelibrary.wiley.com/doi/10.1002/anie.198810211**, (accessed 16 June 2023).
15 D. J. Cram, Cavitands: Organic Hosts with Enforced Cavities, *Science*, 1983, **219**, 1177–1183.
16 B. Dietrich, J. M. Lehn and J.-P. Sauvage, Les Cryptates, *Tetrahedron Lett.*, 1969, **10**, 2889–2892.
17 P. R. Ashton, P. J. Campbell, P. T. Glink, D. Philp, N. Spencer, J. F. Stoddart, E. J. T. Chrystal, S. Menzer, D. J. Williams and P. A. Tasker, Dialkylammonium Ion/Crown Ether Complexes: The Forerunners of a New Family of Interlocked Molecules, *Angew. Chem., Int. Ed. Engl.*, 1995, **34**, 1865–1869.
18 G. Barin, A. Coskun, M. M. G. Fouda and J. F. Stoddart, Mechanically Interlocked Molecules Assembled by π–π Recognition, *ChemPlusChem*, 2012, **77**, 159–185.
19 P. T. Glink, C. Schiavo, J. F. Stoddart and D. J. Williams, The genesis of a new range of interlocked molecules, *Chem. Commun.*, 1996, 1483–1490.
20 J. F. Stoddart, Cyclodextrins, Off-the-Shelf Components for the Construction of Mechanically Interlocked Molecular Systems, *Angew. Chem., Int. Ed. Engl.*, 1992, **31**, 846–848.
21 H. O. Stumpf, Y. Pei, O. Kahn, L. Ouahab and D. Grandjean, A Molecular-Based Magnet with a Fully Interlocked Three-Dimensional Structure, *Science*, 1993, **261**, 447–449.
22 O. Dumele, J. Chen, J. V. Passarelli and S. I. Stupp, Supramolecular Energy Materials, *Adv. Mater.*, 2020, **32**, 1907247.
23 S. Y. An, T. B. Schon, B. T. McAllister and D. S. Seferos, Design strategies for organic carbonyl materials for energy storage: Small molecules, oligomers, polymers and supramolecular structures, *EcoMat*, 2020, **2**, e12055.
24 F. Li, Y. Jiang, B. Zhang, F. Huang, Y. Gao and L. Sun, Towards A Solar Fuel Device: Light-Driven Water Oxidation Catalyzed by a Supramolecular Assembly, *Angew. Chem.*, 2012, **124**, 2467–2470.
25 F. Yu, D. Poole III, S. Mathew, N. Yan, J. Hessels, N. Orth, I. Ivanović-Burmazović and J. N. H. Reek, Control over Electrochemical Water Oxidation Catalysis by Preorganization of Molecular Ruthenium Catalysts in Self-Assembled Nanospheres, *Angew. Chem.*, 2018, **130**, 11417–11421.
26 B. Healy, T. Yu, D. C. da Silva Alves, C. Okeke and C. B. Breslin, Cyclodextrins as Supramolecular Recognition Systems: Applications in the Fabrication of Electrochemical Sensors, *Materials*, 2021, **14**, 1668.
27 A. Kumar, S.-S. Sun and A. J. Lees, Directed assembly metallocyclic supramolecular systems for molecular recognition and chemical sensing, *Coord. Chem. Rev.*, 2008, **252**, 922–939.
28 C. A. Nijhuis, B. J. Ravoo, J. Huskens and D. N. Reinhoudt, Electrochemically controlled supramolecular systems, *Coord. Chem. Rev.*, 2007, **251**, 1761–1780.
29 F. A. Plamper, Polymerizations under electrochemical control, *Colloid Polym. Sci.*, 2014, **292**, 777–783.
30 X. Ma and H. Tian, Stimuli-Responsive Supramolecular Polymers in Aqueous Solution, *Acc. Chem. Res.*, 2014, **47**, 1971–1981.
31 A. Gowda, L. Jacob, D. P. Singh, R. Douali and S. Kumar, Charge Transport in Novel Phenazine Fused Triphenylene Supramolecular Systems, *ChemistrySelect*, 2018, **3**, 6551–6560.
32 H. Chen and J. Fraser Stoddart, From molecular to supramolecular electronics, *Nat. Rev. Mater.*, 2021, **6**, 804–828.
33 J. Idé, R. Méreau, L. Ducasse, F. Castet, Y. Olivier, N. Martinelli, J. Cornil and D. Beljonne, Supramolecular Organization and Charge Transport Properties of Self-Assembled π–π Stacks of Perylene Diimide Dyes, *J. Phys. Chem. B*, 2011, **115**, 5593–5603.
34 L. Motiei, M. Lahav, D. Freeman and M. E. van der Boom, Electrochromic Behavior of a Self-Propagating Molecular-Based Assembly, *J. Am. Chem. Soc.*, 2009, **131**, 3468–3469.
35 B. Tieke, Coordinative supramolecular assembly of electrochromic thin films, *Curr. Opin. Colloid Interface Sci.*, 2011, **16**, 499–507.
36 D. Shimoyama, N. Baser-Kirazli, R. A. Lalancette and F. Jäkle, Electrochromic Polycationic Organoboronium Macrocycles with Multiple Redox States, *Angew. Chem., Int. Ed.*, 2021, **60**, 17942–17946.
37 B. Ding, M. B. Solomon, C. F. Leong and D. M. D'Alessandro, Redox-active ligands: Recent advances towards their incorporation into coordination polymers and metal-organic frameworks, *Coord. Chem. Rev.*, 2021, **439**, 213891.
38 A. Winter, S. Hoeppener, G. R. Newkome and U. S. Schubert, Terpyridine-Functionalized Surfaces: Redox-Active, Switchable, and Electroactive Nanoarchitecturesgland, *Adv. Mater.*, 2011, **23**, 3484–3498.
39 R. Shekurov, V. Khrizanforova, L. Gilmanova, M. Khrizanforov, V. Miluykov, O. Kataeva, Z. Yamaleeva, T. Burganov, T. Gerasimova, A. Khamatgalimov, S. Katsyuba, V. Kovalenko, Y. Krupskaya, V. Kataev,

B. Büchner, V. Bon, I. Senkovska, S. Kaskel, A. Gubaidullin, O. Sinyashin and Y. Budnikova, Zn and Co redox active coordination polymers as efficient electrocatalysts, *Dalton Trans.*, 2019, **48**, 3601–3609.

40 S.-Y. Chou, H. Masai, M. Otani, H. V. Miyagishi, G. Sakamoto, Y. Yamada, Y. Kinoshita, H. Tamiaki, T. Katase, H. Ohta, T. Kondo, A. Nakada, R. Abe, T. Tanaka, K. Uchida and J. Terao, Efficient electrocatalytic H_2O_2 evolution utilizing electron-conducting molecular wires spatially separated by rotaxane encapsulation, *Appl. Catal., B*, 2023, **327**, 122373.

41 S. Suriyakumar, K. Madasamy, M. Kathiresan, M. H. Alkordi and A. M. Stephan, Improved Cycling Performance of Lithium–Sulfur Cell through Supramolecular Interactions, *J. Phys. Chem. C*, 2018, **122**, 27843–27849.

42 B. Ambrose, A. Kannan and M. Kathiresan, Evaluation of negolyte properties of supramolecular binary complexes based on viologen-cucurbit[7]urils, *New J. Chem.*, 2022, **46**, 5606–5613.

43 J. T. Davis, P. A. Gale and R. Quesada, Advances in anion transport and supramolecular medicinal chemistry, *Chem. Soc. Rev.*, 2020, **49**, 6056–6086.

44 L. Imholt, D. Dong, D. Bedrov, I. Cekic-Laskovic, M. Winter and G. Brunklaus, Supramolecular Self-Assembly of Methylated Rotaxanes for Solid Polymer Electrolyte Application, *ACS Macro Lett.*, 2018, **7**, 881–885.

45 T. Kwon, J. W. Choi and A. Coskun, Prospect for Supramolecular Chemistry in High-Energy-Density Rechargeable Batteries, *Joule*, 2019, **3**, 662–682.

46 F. Mo, Q. Li, G. Liang, Y. Zhao, D. Wang, Y. Huang, J. Wei and C. Zhi, A Self-Healing Crease-Free Supramolecular All-Polymer Supercapacitor, *Adv. Sci.*, 2021, **8**, 2100072.

47 X.-Y. Jin, Q. Ge, H. Cong, Y.-Q. Zhang, J.-L. Zhao and N. Jiang, Recent Breakthroughs in Supercapacitors Boosted by Macrocycles, *ChemSusChem*, 2023, **16**, e202300027.

48 L. Feng, R. D. Astumian and J. F. Stoddart, Controlling dynamics in extended molecular frameworks, *Nat. Rev. Chem.*, 2022, **6**, 705–725.

49 Y. Qiu, B. Song, C. Pezzato, D. Shen, W. Liu, L. Zhang, Y. Feng, Q.-H. Guo, K. Cai, W. Li, H. Chen, M. T. Nguyen, Y. Shi, C. Cheng, R. D. Astumian, X. Li and J. F. Stoddart, A precise polyrotaxane synthesizer, *Science*, 2020, **368**, 1247–1253.

50 X.-Y. Chen, H. Chen and J. Fraser Stoddart, The Story of the Little Blue Box: A Tribute to Siegfried Hünig, *Angew. Chem., Int. Ed.*, 2023, **62**, e202211387.

51 C. J. Bruns and J. F. Stoddart, *The Nature of the Mechanical Bond: From Molecules to Machines*, Wiley, 2016, pp. 1–773.

52 C.-W. Chu, D. L. Stares and C. A. Schalley, Light-controlled interconversion between a [c2]daisy chain and a lasso-type pseudo[1]rotaxane, *Chem. Commun.*, 2021, **57**, 12317–12320.

53 Y. Wu, M. Frasconi, W.-G. Liu, R. M. Young, W. A. I. Goddard, M. R. Wasielewski and J. F. Stoddart, Electrochemical Switching of a Fluorescent Molecular Rotor Embedded within a Bistable Rotaxane, *J. Am. Chem. Soc.*, 2020, **142**, 11835–11846.

54 Y.-L. Zhao, W. R. Dichtel, A. Trabolsi, S. Saha, I. Aprahamian and J. F. Stoddart, A Redox-Switchable α-Cyclodextrin-Based [2]Rotaxane, *J. Am. Chem. Soc.*, 2008, **130**, 11294–11296.

55 P. L. Boulas, M. Gómez-Kaifer and L. Echegoyen, Electrochemistry of Supramolecular Systems, *Angew. Chem., Int. Ed.*, 1998, **37**, 216–247.

56 N. Kihara, M. Hashimoto and T. Takata, Redox Behavior of Ferrocene-Containing Rotaxane: Transposition of the Rotaxane Wheel by Redox Reaction of a Ferrocene Moiety Tethered at the End of the Axle, *Org. Lett.*, 2004, **6**, 1693–1696.

57 N. H. Evans, C. J. Serpell and P. D. Beer, A redox-active [3]rotaxane capable of binding and electrochemically sensing chloride and sulfate anions, *Chem. Commun.*, 2011, **47**, 8775–8777.

58 C. Pezzato, M. T. Nguyen, D. J. Kim, O. Anamimoghadam, L. Mosca and J. F. Stoddart, Controlling Dual Molecular Pumps Electrochemically, *Angew. Chem., Int. Ed.*, 2018, **57**, 9325–9329.

59 M. Nandi, S. Bej, S. Bhunia and P. Ghosh, Template Directed Syntheses of Electrochemically Active [2]Rotaxanes: Anion Binding and Redox Studies, *ChemElectroChem*, 2020, **7**, 1038–1047.

60 I. Thomas, Harrison and Shuyen. Harrison, Synthesis of a stable complex of a macrocycle and a threaded chain, *J. Am. Chem. Soc.*, 1967, **89**, 5723–5724.

61 J. A. Bravo, F. M. Raymo, J. F. Stoddart, A. J. P. White and D. J. Williams, High Yielding Template-Directed Syntheses of [2]Rotaxanes, *Eur. J. Org. Chem.*, 1998, 2565–2571.

62 S. D. P. Fielden, D. A. Leigh and S. L. Woltering, Molecular Knots, *Angew. Chem., Int. Ed.*, 2017, **56**, 11166–11194.

63 R. S. Forgan, J.-P. Sauvage and J. F. Stoddart, Chemical Topology: Complex Molecular Knots, Links, and Entanglements, *Chem. Rev.*, 2011, **111**, 5434–5464.

64 P. R. Ashton, C. L. Brown, E. J. T. Chrystal, T. T. Goodnow, A. E. Kaifer, K. P. Parry, D. Philp, A. M. Z. Slawin, N. Spencer, J. F. Stoddart and D. J. Williams, The self-assembly of a highly ordered [2]catenane, *J. Chem. Soc., Chem. Commun.*, 1991, 634–639.

65 M. Cesario, C. O. Dietrich-Buchecker, J. Guilhem, C. Pascard and J. P. Sauvage, Molecular structure of a catenand and its copper(I) catenate: complete rearrangement of the interlocked macrocyclic ligands by complexation, *J. Chem. Soc., Chem. Commun.*, 1985, 244–247.

66 D. Thomas, D. J. Tetlow, Y. Ren, S. Kassem, U. Karaca and D. A. Leigh, Pumping between phases with a pulsed-fuel molecular ratchet, *Nat. Nanotechnol.*, 2022, **17**, 701–707.

67 L. Binks, C. Tian, S. D. P. Fielden, I. J. Vitorica-Yrezabal and D. A. Leigh, Transamidation-Driven Molecular Pumps, *J. Am. Chem. Soc.*, 2022, **144**, 15838–15844.

68 X. Li, A. H. G. David, L. Zhang, B. Song, Y. Jiao, D. Sluysmans, Y. Qiu, Y. Wu, X. Zhao, Y. Feng, L. Mosca and J. F. Stoddart, Fluorescence Quenching by Redox Molecular Pumping, *J. Am. Chem. Soc.*, 2022, **144**, 3572–3579.
69 J. S. W. Seale, B. Song, Y. Qiu and J. F. Stoddart, Precise Non-Equilibrium Polypropylene Glycol Polyrotaxanes, *J. Am. Chem. Soc.*, 2022, **144**, 16898–16904.
70 C. Cheng, P. R. McGonigal, S. T. Schneebeli, H. Li, N. A. Vermeulen, C. Ke and J. F. Stoddart, An artificial molecular pump, *Nat. Nanotechnol.*, 2015, **10**, 547–553.
71 G. Ragazzon, M. Baroncini, S. Silvi, M. Venturi and A. Credi, Light-powered autonomous and directional molecular motion of a dissipative self-assembling system, *Nat. Nanotechnol.*, 2015, **10**, 70–75.
72 S. Corra, M. Curcio and A. Credi, Photoactivated Artificial Molecular Motors, *JACS Au*, 2023, **3**, 1301–1313.
73 L. Andreoni, M. Baroncini, J. Groppi, S. Silvi, C. Taticchi and A. Credi, Photochemical Energy Conversion with Artificial Molecular Machines, *Energy Fuels*, 2021, **35**, 18900–18914.
74 A. Martinez-Cuezva, A. Saura-Sanmartin, M. Alajarin and J. Berna, Mechanically Interlocked Catalysts for Asymmetric Synthesis, *ACS Catal.*, 2020, **10**, 7719–7733.
75 H.-Y. Zhou, Y. Han, Q. Shi and C.-F. Chen, Directional Transportation of a Helic[6]arene along a Nonsymmetric Molecular Axle, *J. Org. Chem.*, 2019, **84**, 5872–5876.
76 I. Aprahamian, The Future of Molecular Machines, *ACS Cent. Sci.*, 2020, **6**, 347–358.
77 F. B. L. Cougnon, A. R. Stefankiewicz and S. Ulrich, Dynamic covalent synthesis, *Chem. Sci.*, 2024, **15**, 879–895.
78 Q.-H. Guo, Y. Qiu, X. Kuang, J. Liang, Y. Feng, L. Zhang, Y. Jiao, D. Shen, R. D. Astumian and J. F. Stoddart, Artificial Molecular Pump Operating in Response to Electricity and Light, *J. Am. Chem. Soc.*, 2020, **142**, 14443–14449.
79 Y. Qiu, L. Zhang, C. Pezzato, Y. Feng, W. Li, M. T. Nguyen, C. Cheng, D. Shen, Q.-H. Guo, Y. Shi, K. Cai, F. M. Alsubaie, R. D. Astumian and J. F. Stoddart, A Molecular Dual Pump, *J. Am. Chem. Soc.*, 2019, **141**, 17472–17476.
80 A. Credi, M. Semeraro, S. Silvi and M. Venturi, Redox Control of Molecular Motion in Switchable Artificial Nanoscale Devices, *Antioxid. Redox Signal.*, 2011, **14**, 1119–1165.
81 H.-R. Tseng, S. A. Vignon and J. F. Stoddart, Toward Chemically Controlled Nanoscale Molecular Machinery, *Angew. Chem., Int. Ed.*, 2003, **42**, 1491–1495.
82 H. V. Schröder and C. A. Schalley, Electrochemically switchable rotaxanes: recent strides in new directions, *Chem. Sci.*, 2019, **10**, 9626–9639.
83 M. Franz, J. A. Januszewski, D. Wendinger, C. Neiss, L. D. Movsisyan, F. Hampel, H. L. Anderson, A. Görling and R. R. Tykwinski, Cumulene Rotaxanes: Stabilization and Study of [9]Cumulenes, *Angew. Chem., Int. Ed.*, 2015, **54**, 6645–6649.
84 A. Ulfkjær, F. W. Nielsen, H. Al-Kerdi, T. Ruß, Z. K. Nielsen, J. Ulstrup, L. Sun, K. Moth-Poulsen, J. Zhang and M. Pittelkow, A gold-nanoparticle stoppered [2]rotaxane, *Nanoscale*, 2018, **10**, 9133–9140.
85 H. V. Schröder, H. Hupatz, A. J. Achazi, S. Sobottka, B. Sarkar, B. Paulus and C. A. Schalley, A Divalent Pentastable Redox-Switchable Donor–Acceptor Rotaxane, *Chem. – Eur. J.*, 2017, **23**, 2960–2967.
86 Cyclic Voltammetry—"Electrochemical Spectroscopy". New Analytical Methods (25) – Heinze – 1984 – Angewandte Chemie International Edition in English – Wiley Online Library, **https://onlinelibrary.wiley.com/doi/10.1002/anie.198408313**, (accessed 6 July 2023).
87 Y. Qiu, B. Song, C. Pezzato, D. Shen, W. Liu, L. Zhang, Y. Feng, Q.-H. Guo, K. Cai, W. Li, H. Chen, M. T. Nguyen, Y. Shi, C. Cheng, R. D. Astumian, X. Li and J. F. Stoddart, A precise polyrotaxane synthesizer, *Science*, 2020, **368**, 1247–1253.
88 R. A. Bissell, E. Córdova, A. E. Kaifer and J. F. Stoddart, A chemically and electrochemically switchable molecular shuttle, *Nature*, 1994, **369**, 133–137.
89 Supramolecular Electrochemistry | Wiley, **https://www.wiley.com/en-us/Supramolecular+Electrochemistry-p-9783527613618**, (accessed 6 July 2023).
90 Analytical Methods in Supramolecular Chemistry, 2nd, Completely Revised and Enlarged Edition | Wiley, **https://www.wiley.com/en-gb/Analytical+Methods+in+Supramolecular+Chemistry%2C+2nd%2C+Completely+Revised+and+Enlarged+Edition-p-9783527329823**, (accessed 24 September 2023).
91 A. Altieri, F. G. Gatti, E. R. Kay, D. A. Leigh, D. Martel, F. Paolucci, A. M. Z. Slawin and J. K. Y. Wong, Electrochemically Switchable Hydrogen-Bonded Molecular Shuttles, *J. Am. Chem. Soc.*, 2003, **125**, 8644–8654.
92 J. F. Stoddart, Mechanically Interlocked Molecules (MIMs)—Molecular Shuttles, Switches, and Machines (Nobel Lecture), *Angew. Chem., Int. Ed.*, 2017, **56**, 11094–11125.
93 K. Cai, Y. Shi, G.-W. Zhuang, L. Zhang, Y. Qiu, D. Shen, H. Chen, Y. Jiao, H. Wu, C. Cheng and J. F. Stoddart, Molecular-Pump-Enabled Synthesis of a Daisy Chain Polymer, *J. Am. Chem. Soc.*, 2020, **142**, 10308–10313.
94 S. Durot, F. Reviriego and J.-P. Sauvage, Copper-complexed catenanes and rotaxanes in motion: 15 years of molecular machines, *Dalton Trans.*, 2010, **39**, 10557–10570.
95 E. R. Kay, D. A. Leigh and F. Zerbetto, Synthetic Molecular Motors and Mechanical Machines, *Angew. Chem., Int. Ed.*, 2007, **46**, 72–191.
96 D. Leigh, *Nature*, 2007, **445**, xi–xi.
97 Y. Jiao, Y. Qiu, L. Zhang, W.-G. Liu, H. Mao, H. Chen, Y. Feng, K. Cai, D. Shen, B. Song, X.-Y. Chen, X. Li, X. Zhao, R. M. Young, C. L. Stern, M. R. Wasielewski, R. D. Astumian, W. A. Goddard and J. F. Stoddart, Electron-catalysed molecular recognition, *Nature*, 2022, **603**, 265–270.
98 X.-H. Gu, J.-X. Yang, L.-J. Liu, Y. Hai, T.-G. Zhan and K.-D. Zhang, A light- and redox-switchable tristable [3]

rotaxane with orthogonal controllable shuttling of different wheels, *New J. Chem.*, 2023, **47**, 19767–19774.

99 J. Echavarren, M. A. Y. Gall, A. Haertsch, D. A. Leigh, V. Marcos and D. J. Tetlow, Active template rotaxane synthesis through the Ni-catalyzed cross-coupling of alkylzinc reagents with redox-active esters, *Chem. Sci.*, 2019, **10**, 7269–7273.

100 S. Bej, M. Nandi, T. K. Ghosh and P. Ghosh, Cu(II) templated formation of [n]pseudorotaxanes (n = 2, 3, 4) using a tris-amino ether macrocyclic wheel and multidentate axles, *Dalton Trans.*, 2019, **48**, 6853–6862.

101 J. E. M. Lewis, P. D. Beer, S. J. Loeb and S. M. Goldup, Metal ions in the synthesis of interlocked molecules and materials, *Chem. Soc. Rev.*, 2017, **46**, 2577–2591.

102 L. Fang, M. A. Olson, D. Benítez, E. Tkatchouk, W. A. G. Iii and J. F. Stoddart, Mechanically bonded macromolecules, *Chem. Soc. Rev.*, 2009, **39**, 17–29.

103 G. J. E. Davidson, S. Sharma and S. J. Loeb, A [2]Rotaxane Flip Switch Driven by Coordination Geometry, *Angew. Chem., Int. Ed.*, 2010, **49**, 4938–4942.

104 M. R. Panman, B. H. Bakker, D. den Uyl, E. R. Kay, D. A. Leigh, W. J. Buma, A. M. Brouwer, J. A. J. Geenevasen and S. Woutersen, Water lubricates hydrogen-bonded molecular machines, *Nat. Chem.*, 2013, **5**, 929–934.

105 J. Y. C. Lim and P. D. Beer, Electrochemical Bromide Sensing with a Halogen Bonding [2]Rotaxane, *Eur. J. Org. Chem.*, 2019, 3433–3441.

106 H. Fu, X. Shao, C. Chipot and W. Cai, The lubricating role of water in the shuttling of rotaxanes, *Chem. Sci.*, 2017, **8**, 5087–5094.

107 A.-J. Avestro, M. E. Belowich and J. F. Stoddart, Cooperative self-assembly: producing synthetic polymers with precise and concise primary structures, *Chem. Soc. Rev.*, 2012, **41**, 5881–5895.

108 S. Du, H. Fu, X. Shao, C. Chipot and W. Cai, Water-Controlled Switching in Rotaxanes, *J. Phys. Chem. C*, 2018, **122**, 9229–9234.

109 J. J. Danon, D. A. Leigh, P. R. McGonigal, J. W. Ward and J. Wu, Triply Threaded [4]Rotaxanes, *J. Am. Chem. Soc.*, 2016, **138**, 12643–12647.

110 P. E. Barran, H. L. Cole, S. M. Goldup, D. A. Leigh, P. R. McGonigal, M. D. Symes, J. Wu and M. Zengerle, Active-Metal Template Synthesis of a Molecular Trefoil Knot, *Angew. Chem., Int. Ed.*, 2011, **50**, 12280–12284.

111 E. A. Neal and S. M. Goldup, Competitive formation of homocircuit [3]rotaxanes in synthetically useful yields in the bipyridine-mediated active template CuAAC reaction, *Chem. Sci.*, 2015, **6**, 2398–2404.

112 H. Lahlali, K. Jobe, M. Watkinson and S. M. Goldup, Macrocycle Size Matters: "Small" Functionalized Rotaxanes in Excellent Yield Using the CuAAC Active Template Approach, *Angew. Chem., Int. Ed.*, 2011, **50**, 4151–4155.

113 Y. Wang, T. Cheng, J. Sun, Z. Liu, M. Frasconi, W. A. I. Goddard and J. F. Stoddart, Neighboring Component Effect in a Tri-stable [2]Rotaxane, *J. Am. Chem. Soc.*, 2018, **140**, 13827–13834.

114 R. M. Stephenson, X. Wang, A. Coskun, J. F. Stoddart and J. I. Zink, Excited state distortions in a charge transfer state of a donor–acceptor [2]rotaxane, *Phys. Chem. Chem. Phys.*, 2010, **12**, 14135–14143.

115 S. K. Dey, A. Coskun, A. C. Fahrenbach, G. Barin, A. N. Basuray, A. Trabolsi, Y. Y. Botros and J. F. Stoddart, A redox-active reverse donor–acceptor bistable [2]rotaxane, *Chem. Sci.*, 2011, **2**, 1046–1053.

116 X. Li, J. Y. C. Lim and P. D. Beer, Acid-Regulated Switching of Metal Cation and Anion Guest Binding in Halogen-Bonding Rotaxanes, *Chem. – Eur. J.*, 2018, **24**, 17788–17795.

117 D.-H. Qu and H. Tian, Novel and efficient templates for assembly of rotaxanes and catenanes, *Chem. Sci.*, 2011, **2**, 1011–1015.

118 M. J. Langton, Y. Xiong and P. D. Beer, Active-Metal Template Synthesis of a Halogen-Bonding Rotaxane for Anion Recognition, *Chem. – Eur. J.*, 2015, **21**, 18910–18914.

119 M. Cirulli, A. Kaur, J. E. M. Lewis, Z. Zhang, J. A. Kitchen, S. M. Goldup and M. M. Roessler, Rotaxane-Based Transition Metal Complexes: Effect of the Mechanical Bond on Structure and Electronic Properties, *J. Am. Chem. Soc.*, 2019, **141**, 879–889.

120 J. M. Van Raden, N. N. Jarenwattananon, L. N. Zakharov and R. Jasti, Active Metal Template Synthesis and Characterization of a Nanohoop [c2]Daisy Chain Rotaxane, *Chem. – Eur. J.*, 2020, **26**, 10205–10209.

121 S. W. Hewson and K. M. Mullen, Porphyrin-Containing Rotaxane Assemblies, *Eur. J. Org. Chem.*, 2019, 3358–3370.

122 L. Zhang, Y. Qiu, W.-G. Liu, H. Chen, D. Shen, B. Song, K. Cai, H. Wu, Y. Jiao, Y. Feng, J. S. W. Seale, C. Pezzato, J. Tian, Y. Tan, X.-Y. Chen, Q.-H. Guo, C. L. Stern, D. Philp, R. D. Astumian, W. A. Goddard and J. F. Stoddart, An electric molecular motor, *Nature*, 2023, **613**, 280–286.

123 L. Feng, Y. Qiu, Q.-H. Guo, Z. Chen, J. S. W. Seale, K. He, H. Wu, Y. Feng, O. K. Farha, R. D. Astumian and J. F. Stoddart, Active mechanisorption driven by pumping cassettes, *Science*, 2021, **374**, 1215–1221.

124 S. Amano, S. D. P. Fielden and D. A. Leigh, A catalysis-driven artificial molecular pump, *Nature*, 2021, **594**, 529–534.

125 H. V. Schröder, F. Stein, J. M. Wollschläger, S. Sobottka, M. Gaedke, B. Sarkar and C. A. Schalley, Accordion-Like Motion in Electrochemically Switchable Crown Ether/Ammonium Oligorotaxanes, *Angew. Chem., Int. Ed.*, 2019, **58**, 3496–3500.

126 C. Biagini, S. D. P. Fielden, D. A. Leigh, F. Schaufelberger, S. Di Stefano and D. Thomas, Dissipative Catalysis with a Molecular Machine, *Angew. Chem., Int. Ed.*, 2019, **58**, 9876–9880.

127 S. Erbas-Cakmak, S. D. P. Fielden, U. Karaca, D. A. Leigh, C. T. McTernan, D. J. Tetlow and M. R. Wilson, Rotary and

linear molecular motors driven by pulses of a chemical fuel, *Science*, 2017, **358**, 340–343.
128 E. A. Neal and S. M. Goldup, Chemical consequences of mechanical bonding in catenanes and rotaxanes: isomerism, modification, catalysis and molecular machines for synthesis, *Chem. Commun.*, 2014, **50**, 5128–5142.
129 D. A. Leigh, V. Marcos and M. R. Wilson, Rotaxane Catalysts, *ACS Catal.*, 2014, **4**, 4490–4497.
130 C. J. Bruns and J. F. Stoddart, Rotaxane-Based Molecular Muscles, *Acc. Chem. Res.*, 2014, **47**, 2186–2199.
131 M. Dumartin, M. C. Lipke and J. F. Stoddart, A Redox-Switchable Molecular Zipper, *J. Am. Chem. Soc.*, 2019, **141**, 18308–18317.
132 A. Goujon, E. Moulin, G. Fuks and N. Giuseppone, [c2] Daisy Chain Rotaxanes as Molecular Muscles, *CCS Chem.*, 2019, **1**, 83–96.
133 A. Goujon, T. Lang, G. Mariani, E. Moulin, G. Fuks, J. Raya, E. Buhler and N. Giuseppone, Bistable [c2] Daisy Chain Rotaxanes as Reversible Muscle-like Actuators in Mechanically Active Gels, *J. Am. Chem. Soc.*, 2017, **139**, 14825–14828.
134 C. J. Bruns, M. Frasconi, J. Iehl, K. J. Hartlieb, S. T. Schneebeli, C. Cheng, S. I. Stupp and J. F. Stoddart, Redox Switchable Daisy Chain Rotaxanes Driven by Radical–Radical Interactions, *J. Am. Chem. Soc.*, 2014, **136**, 4714–4723.
135 K. Cai, B. Cui, B. Song, H. Wang, Y. Qiu, L. O. Jones, W. Liu, Y. Shi, S. Vemuri, D. Shen, T. Jiao, L. Zhang, H. Wu, H. Chen, Y. Jiao, Y. Wang, C. L. Stern, H. Li, G. C. Schatz, X. Li and J. F. Stoddart, Radical Cyclic [3] Daisy Chains, *Chem*, 2021, **7**, 174–189.
136 S. S. Andersen, A. W. Saad, R. Kristensen, T. S. Pedersen, L. J. O'Driscoll, A. H. Flood and J. O. Jeppesen, Salts accelerate the switching kinetics of a cyclobis(paraquat- p -phenylene) [2]rotaxane, *Org. Biomol. Chem.*, 2019, **17**, 2432–2441.
137 N. H. Evans, Recent Advances in the Synthesis and Application of Hydrogen Bond Templated Rotaxanes and Catenanes, *Eur. J. Org. Chem.*, 2019, 3320–3343.
138 P. R. Ashton, D. Philp, M. V. Reddington, A. M. Z. Slawin, N. Spencer, J. F. Stoddart and D. J. Williams, The self-assembly of complexes with [2]pseudorotaxane superstructures, *J. Chem. Soc., Chem. Commun.*, 1991, 1680–1683.
139 F. M. Menger, Supramolecular chemistry and self-assembly, *Proc. Natl. Acad. Sci. U. S. A.*, 2002, **99**, 4818–4822.
140 J. L. Atwood and J.-M. Lehn, *Comprehensive supramolecular chemistry*, Pergamon, New York, 1st edn, 1996.
141 D. Philp and J. F. Stoddart, Self-Assembly in Natural and Unnatural Systems, *Angew. Chem., Int. Ed. Engl.*, 1996, **35**, 1154–1196.
142 D. Phlip, Supramolecular chemistry: Concepts and perspectives. By J.-M. Lehn, VCH, Weinheim 1995, x, 271 pp., softcover, DM 58.00, ISBN 3-527-2931 1-6, *Adv. Mater.*, 1996, **8**, 866–868.
143 E. R. Kay, D. A. Leigh and F. Zerbetto, Synthetic Molecular Motors and Mechanical Machines, *Angew. Chem., Int. Ed.*, 2007, **46**, 72–191.
144 V. Balzani, A. Credi, S. Silvi and M. Venturi, Artificial nanomachines based on interlocked molecular species: recent advances, *Chem. Soc. Rev.*, 2006, **35**, 1135–1149.
145 H. Tian and Q.-C. Wang, Recent progress on switchable rotaxanes, *Chem. Soc. Rev.*, 2006, **35**, 361–374.
146 S. Saha and J. F. Stoddart, Photo-driven molecular devices, *Chem. Soc. Rev.*, 2006, **36**, 77–92.
147 B. Champin, P. Mobian and J.-P. Sauvage, Transition metal complexes as molecular machine prototypes, *Chem. Soc. Rev.*, 2007, **36**, 358–366.
148 H. Marubayashi, M. Ebe, A. Imasaki, K. Fujiwara, N. Mashita, K. Hagita, T. Murashima, S. Mori, T. Isono, T. Satoh and H. Jinnai, Toughening of a polymer network by the addition of a small amount of large-sized multicyclic chains, *Polymer*, 2024, **292**, 126607.
149 B. H. Wilson and S. J. Loeb, Integrating the Mechanical Bond into Metal-Organic Frameworks, *Chem*, 2020, **6**, 1604–1612.
150 T. Ma, Y. Zhou, C. S. Diercks, J. Kwon, F. Gándara, H. Lyu, N. Hanikel, P. Pena-Sánchez, Y. Liu, N. J. Diercks, R. O. Ritchie, D. M. Proserpio, O. Terasaki and O. M. Yaghi, Catenated covalent organic frameworks constructed from polyhedra, *Nat. Synth.*, 2023, **2**, 286–295.
151 M.-Y. Guo, G. Li, S.-L. Yang, R. Bu, X.-Q. Piao and E.-Q. Gao, Metal-Organic Frameworks with Novel Catenane-like Interlocking: Metal-Determined Photoresponse and Uranyl Sensing, *Chem. – Eur. J.*, 2021, **27**, 16415–16421.
152 Y.-G. Huang, S.-Q. Wu, W.-H. Deng, G. Xu, F.-L. Hu, J. P. Hill, W. Wei, S.-Q. Su, L. K. Shrestha, O. Sato, M.-Y. Wu, M.-C. Hong and K. Ariga, Selective CO2 Capture and High Proton Conductivity of a Functional Star-of-David Catenane Metal–Organic Framework, *Adv. Mater.*, 2017, **29**, 1703301.
153 G. Gil-Ramírez, D. A. Leigh and A. J. Stephens, Catenanes: Fifty Years of Molecular Links, *Angew. Chem., Int. Ed.*, 2015, **54**, 6110–6150.
154 K. E. Griffiths and J. F. Stoddart, Template-directed synthesis of donor/acceptor [2]catenanes and [2]rotaxanes, *Pure Appl. Chem.*, 2008, **80**, 485–506.
155 E. R. Kay and D. A. Leigh, in *Molecular Machines*, ed. T. R. Kelly, Springer, Berlin, Heidelberg, 2005, pp. 133–177.
156 J.-P. Collin, C. Dietrich-Buchecker, P. Gaviña, M. C. Jimenez-Molero and J.-P. Sauvage, Shuttles and Muscles: Linear Molecular Machines Based on Transition Metals, *Acc. Chem. Res.*, 2001, **34**, 477–487.
157 C. O. Dietrich-Buchecker, M. C. Jimenez-Molero, V. Sartor and J.-P. Sauvage, Rotaxanes and catenanes as prototypes of molecular machines and motors, *Pure Appl. Chem.*, 2003, **75**, 1383–1393.
158 J.-P. Collin, V. Heitz and J.-P. Sauvage, in *Molecular Machines*, ed. T. R. Kelly, Springer, Berlin, Heidelberg, 2005, pp. 29–62.

159 J.-P. Sauvage, Transition Metal-Containing Rotaxanes and Catenanes in Motion: Toward Molecular Machines and Motors, *Acc. Chem. Res.*, 1998, **31**, 611–619.
160 E. Wasserman, Chemical Topology, *Sci. Am.*, 1962, **207**, 94–106.
161 M. T. Nguyen, D. P. Ferris, C. Pezzato, Y. Wang and J. F. Stoddart, Densely Charged Dodecacationic [3]- and Tetracosacationic Radial [5]Catenanes, *Chem*, 2018, **4**, 2329–2344.
162 J. C. Barnes, A. C. Fahrenbach, D. Cao, S. M. Dyar, M. Frasconi, M. A. Giesener, D. Benítez, E. Tkatchouk, O. Chernyashevskyy, W. H. Shin, H. Li, S. Sampath, C. L. Stern, A. A. Sarjeant, K. J. Hartlieb, Z. Liu, R. Carmieli, Y. Y. Botros, J. W. Choi, A. M. Z. Slawin, J. B. Ketterson, M. R. Wasielewski, W. A. Goddard and J. F. Stoddart, A Radically Configurable Six-State Compound, *Science*, 2013, **339**, 429–433.
163 J. Sun, Z. Liu, W.-G. Liu, Y. Wu, Y. Wang, J. C. Barnes, K. R. Hermann, W. A. I. Goddard, M. R. Wasielewski and J. F. Stoddart, Mechanical-Bond-Protected, Air-Stable Radicals, *J. Am. Chem. Soc.*, 2017, **139**, 12704–12709.
164 C.-Y. Wang, G. Wu, J. Zhu, T. Jiao, Y. Zhang and H. Li, An Octacationic [2]Catenane Formed by Oxime Condensation: A Bistable Molecular Switch, *ChemPlusChem*, 2020, **85**, 84–87.
165 K. S. Chichak, S. J. Cantrill, A. R. Pease, S.-H. Chiu, G. W. V. Cave, J. L. Atwood and J. F. Stoddart, Molecular Borromean Rings, *Science*, 2004, **304**, 1308–1312.
166 J. J. Danon, A. Krüger, D. A. Leigh, J.-F. Lemonnier, A. J. Stephens, I. J. Vitorica-Yrezabal and S. L. Woltering, Braiding a molecular knot with eight crossings, *Science*, 2017, **355**, 159–162.
167 B. Lewandowski, G. De Bo, J. W. Ward, M. Papmeyer, S. Kuschel, M. J. Aldegunde, P. M. E. Gramlich, D. Heckmann, S. M. Goldup, D. M. D'Souza, A. E. Fernandes and D. A. Leigh, Sequence-Specific Peptide Synthesis by an Artificial Small-Molecule Machine, *Science*, 2013, **339**, 189–193.
168 G. De Bo, M. A. Y. Gall, S. Kuschel, J. De Winter, P. Gerbaux and D. A. Leigh, An artificial molecular machine that builds an asymmetric catalyst, *Nat. Nanotechnol.*, 2018, **13**, 381–385.
169 J. Berná, D. A. Leigh, M. Lubomska, S. M. Mendoza, E. M. Pérez, P. Rudolf, G. Teobaldi and F. Zerbetto, Macroscopic transport by synthetic molecular machines, *Nat. Mater.*, 2005, **4**, 704–710.
170 T. Ashirov and A. Coskun, The Power of the Mechanical Bond, *Chem*, 2018, **4**, 2260–2262.
171 E. R. Kay and D. A. Leigh, Rise of the Molecular Machines, *Angew. Chem., Int. Ed.*, 2015, **54**, 10080–10088.
172 M. Baroncini, L. Casimiro, C. de Vet, J. Groppi, S. Silvi and A. Credi, Making and Operating Molecular Machines: A Multidisciplinary Challenge, *ChemistryOpen*, 2018, **7**, 169–179.
173 A. W. Heard and S. M. Goldup, Simplicity in the Design, Operation, and Applications of Mechanically Interlocked Molecular Machines, *ACS Cent. Sci.*, 2020, **6**, 117–128.
174 Q. Wang, D. Chen and H. Tian, Artificial molecular machines that can perform work, *Sci. China: Chem.*, 2018, **61**, 1261–1273.
175 M. Nandi, S. Bej and P. Ghosh, NDI-integrated rotaxane/catenane and their interactions with anions, *Dalton Trans.*, 2022, **51**, 13507–13514.
176 N. Pairault and J. Niemeyer, Chiral Mechanically Interlocked Molecules – Applications of Rotaxanes, Catenanes and Molecular Knots in Stereoselective Chemosensing and Catalysis, *Synlett*, 2018, 689–698.
177 N. H. Evans, Chiral Catenanes and Rotaxanes: Fundamentals and Emerging Applications, *Chem. – Eur. J.*, 2018, **24**, 3101–3112.
178 H. Yu Au-Yeung and Y. Deng, Distinctive features and challenges in catenane chemistry, *Chem. Sci.*, 2022, **13**, 3315–3334.
179 J. M. Van Raden, B. M. White, L. N. Zakharov and R. Jasti, Nanohoop Rotaxanes from Active Metal Template Syntheses and Their Potential in Sensing Applications, *Angew. Chem., Int. Ed.*, 2019, **58**, 7341–7345.
180 P. Wu, B. Dharmadhikari, P. Patra and X. Xiong, Rotaxane nanomachines in future molecular electronics, *Nanoscale Adv.*, 2022, **4**, 3418–3461.
181 C. Yang and H. Chen, A Roadmap for Mechanically Interlocked Molecular Junctions at Nanoscale, *ACS Appl. Nano Mater.*, 2022, **5**, 13874–13886.
182 G. Zhang, C. Xie, P. You and S. Li, in *Introduction to Organic Electronic Devices*, ed. G. Zhang, C. Xie, P. You and S. Li, Springer Nature, Singapore, 2022, pp. 261–281.
183 N. H. Pérez, P. S. Sherin, V. Posligua, J. L. Greenfield, M. J. Fuchter, K. E. Jelfs, M. K. Kuimova and J. E. M. Lewis, Emerging properties from mechanical tethering within a post-synthetically functionalised catenane scaffold, *Chem. Sci.*, 2022, **13**, 11368–11375.
184 G. Yu, B. C. Yung, Z. Zhou, Z. Mao and X. Chen, Artificial Molecular Machines in Nanotheranostics, *ACS Nano*, 2018, **12**, 7–12.
185 P. Rajalakshmi, D. N. Peter, S. Jesu Johnson and N. Ananthi, Structure-Activity Relationship of Supramolecular Compounds in Drug Delivery, *Mini-Rev. Org. Chem.*, 2021, **18**, 961–989.
186 A. S. Braegelman and M. J. Webber, Integrating Stimuli-Responsive Properties in Host-Guest Supramolecular Drug Delivery Systems, *Theranostics*, 2019, **9**, 3017–3040.
187 K. Zhu, G. Baggi and S. J. Loeb, Ring-through-ring molecular shuttling in a saturated [3]rotaxane, *Nat. Chem.*, 2018, **10**, 625–630.
188 S. Du, H. Liu, X. Shao, C. Chipot and W. Cai, Free-Energy Landscape of Stepwise, Directional Motion in Multiple Molecular Switches, *J. Phys. Chem. C*, 2020, **124**, 6448–6453.

189 T. Takata, Switchable Polymer Materials Controlled by Rotaxane Macromolecular Switches, *ACS Cent. Sci.*, 2020, **6**, 129–143.
190 A. W. Heard, J. M. Suárez and S. M. Goldup, Controlling catalyst activity, chemoselectivity and stereoselectivity with the mechanical bond, *Nat. Rev. Chem.*, 2022, **6**, 182–196.
191 A. Bessaguet, Q. Blancart-Remaury, P. Poinot, I. Opalinski and S. Papot, Stimuli-Responsive Catenane-Based Catalysts, *Angew. Chem., Int. Ed.*, 2023, **62**, e202216787.
192 S. Kundu, D. Mondal, E. Elramadi, I. Valiyev and M. Schmittel, Parallel Allosteric Inhibition of Shuttling Motion and Catalysis in a Silver(I)-loaded [2]Rotaxane, *Org. Lett.*, 2022, **24**, 6609–6613.